




Climatology of Transient Luminous Events and Lightning Observed Above Europe and the Mediterranean Sea

Enrico Arnone^{1,2}  · József Bór³ · Olivier Chanrion⁴ · Veronika Barta³ · Stefano Dietrich² · Carl-Fredrik Enell⁵ · Thomas Farges⁶ · Martin Füllekrug⁷ · Antti Kero⁸ · Roberto Labanti⁹ · Antti Mäkelä¹⁰ · Keren Mezuman^{11,12} · Anna Odzimek¹³ · Martin Popek¹⁴ · Marco Prevedelli¹⁵ · Marco Ridolfi^{15,16} · Serge Soula¹⁷ · Diego Valeri¹⁸ · Oscar van der Velde¹⁹ · Yoav Yair²⁰ · Ferruccio Zanotti⁹ · Przemyslaw Zoladek²¹ · Torsten Neubert⁴

Received: 16 April 2019 / Accepted: 25 September 2019 / Published online: 4 November 2019
© Springer Nature B.V. 2019

Abstract

In 1999, the first sprites were observed above European thunderstorms using sensitive cameras. Since then, Eurosprite campaigns have been conducted to observe sprites and other transient luminous events (TLEs), expanding into a network covering large parts of Europe and coastal areas. In 2009 through 2013, the number of optical observations of TLEs reached a peak of 2000 per year. Because of this unprecedented number of European observations, it was possible to construct a climatology of 8394 TLEs observed above 1018 thunderstorm systems and study for the first time their distribution and seasonal cycle above Europe and parts of the Mediterranean Sea. The number of TLEs per thunderstorm was found to follow a power law, with less than 10 TLEs for 801 thunderstorms and up to 195 TLEs above the most prolific one. The majority of TLEs were classified as sprites, 641 elves, 280 halos, 70 upward lightning, 2 blue jets and 1 gigantic jet. The climatology shows intense TLE activity during summer over continental areas and in late autumn over coastal areas and sea. The two seasons peak, respectively, in August and November, separated by March and April with almost no TLEs, and a relative minimum around September. The observed TLE activity, i.e. mostly sprites, is shown to be largely consistent with lightning activity, with a 1/1000 of observed TLE-to-lightning ratio in regions with most observations. The overall behaviour is consistent among individual years, making the observed seasonal cycle a robust general feature of TLE activity above Europe.

Keywords Thunderstorms · Lightning · Transient luminous events · Ground-based observations · Europe · Climatology

✉ Enrico Arnone
enrico.arnone@unito.it

1 Introduction

1.1 Transient Luminous Events

Three decades ago, a test low-light camera recorded a sprite (Franz et al. 1990), a spectacular discharge extending for tens of km above a thunderstorm. It was the first discovery of a whole family of upper atmosphere electrical processes, collectively known as transient luminous events (TLEs—see reviews by Rodger 1999; Neubert 2003; Füllekrug et al. 2006; Neubert et al. 2008; Pasko et al. 2011). TLEs occur in the region between the upper troposphere and the mesopause, between the top of thunderclouds and the lower ionosphere. They are the visible manifestation of the electrical impact of thunderstorms onto the above atmosphere. They can be made of streamers, weakly ionized plasma channels (Petrov and Petrova 1999; Ebert et al. 2006; Luque and Ebert 2009), roughly up to 70 km altitude; or be large diffused patches of enhanced ionization at higher altitude, where the dielectric relaxation timescale becomes comparable with that of dissociative attachment (Pasko et al. 1998). Over the years, TLEs have been distinguished in specific classes: blue jets (Wescott et al. 1995; Boeck et al. 1995; Petrov and Petrova 1999) are fountain-like streamers directly expanding from their leader core and injected from the thundercloud top up to 40 km altitude towards the ionosphere (Krehbiel et al. 2008; Pasko 2008). Sprites (Sentman and Wescott 1993; Lyons 1994; Sentman et al. 1995) are luminous discharges that initiate at about 70 km altitude (Stenbaek-Nielsen et al. 2010) as a consequence of the transient quasi-electrostatic field induced by large positive cloud-to-ground (+ CG) lightning strokes (Pasko et al. 1997). They extend downwards to 40 km as streamers and upwards to 90 km altitude as diffuse emission and are tens of km wide (Stenbaek-Nielsen et al. 2000). Sprite halos occur as downward moving diffuse glow at 70–80 km altitude, often accompanying sprite events but in some occasions alone (Barrington Leigh et al. 2001; Wescott et al. 2001). Elves appear as horizontally expanding diffuse emission rings of a few hundreds km diameter at about 90 km altitude, when the electromagnetic pulse of a triggering lightning stroke hits the lower ionosphere (Boeck et al. 1992; Fuku-nishi et al. 1996; Inan et al. 1997). Much rarer are gigantic jets (GJs), which join together apparent features of blue jets and sprites, and cause a direct connection of the thunderstorm to the lower ionosphere (Pasko et al. 2002; Su et al. 2003; Cummer et al. 2009; van der Velde et al. 2010a). Depending on the relaxation timescales at the altitude of occurrence, TLEs last from several hundreds of milliseconds (jets) down to a few milliseconds (elves). Sprites are the most commonly observed kind of TLE from ground-based video observations, with global occurrence rate of about 1–3 sprite min^{-1} (Ignaccolo et al. 2008, and references therein). Satellite observations (Chen et al. 2008) confirmed a global occurrence rate of sprites of about 1 per minute, a similar rate for halos, whereas the much higher efficiency in observing elves led to an estimate of about 30 elve min^{-1} globally. A high elve/sprite ratio (6:1) was found also by adopting data from ground-based photometers, further pointing to a selection bias towards sprites in ground-based video observations (Newsome and Inan 2010).

1.2 Eurosprite: A Review of European TLE Observations

Europe is a unique region for studies of TLEs under extremely varying conditions. The first images of European TLEs were captured by chance in 1999 over the Balkans from

an aircraft based camera during the 999 Leonids-MAC airborne campaign (Gardner and Taylor, Second Leonids-MAC workshop, Tel Aviv, 2000). The first dedicated observations were obtained in 2000 with a camera installed at the Observatoire Midi-Pyrénées, located at Pic du Midi in the French Pyrenees (Neubert et al. 2001). The authors recorded 40 sprites over the Alps and Southern France, in connection with cold fronts coming from the Atlantic. In the following years, Eurosprite campaigns were conducted during summer leading to over 700 TLE images being captured in the period from 2000 to 2008 (Neubert et al. 2005, 2008; Chanrion et al. 2007; Arnone et al. 2008b). The network involves also several non-optical correlative measurements widely adopted for further insight into the physics of the observed TLEs: a broad range of correlative measurements including ELF-VLF radio and infrasound recording (Price et al. 2002; Greenberg and Price 2004; Liszka and Hobara 2006; Neubert et al. 2008; Farges and Blanc 2010; Sători et al. 2013). These campaigns allowed a great number of detailed studies using specific European TLE events and thunderstorms. This includes investigations of radio signatures of TLEs and thunderstorm-induced effects on the atmosphere (Haldoupis et al. 2004, 2006, 2010; Mika et al. 2005, 2006; Farges et al. 2007; Greenberg et al. 2009; NaitAmor et al. 2010; Füllekrug et al. 2010, 2011); investigations on infrasound signatures of sprites (Farges et al. 2005; Ignaccolo et al. 2008; Farges and Blanc 2010); meteorology of TLEs and of their producing thunderstorm (Ignaccolo et al. 2006; van der Velde et al. 2006, 2010b; Ganot et al. 2007; Bór et al. 2009, 2018; Iwański et al. 2009; Savtchenko et al. 2009; Vadislavsky et al. 2009; Yair et al. 2009; Soula et al. 2010; Mäkelä et al. 2010); the morphological aspects of various sprite types (Bór 2013). A general collection of research related to Eurosprite was included in Füllekrug et al. (2006) and presented by Neubert et al. (2008).

Eurosprite has since then expanded to become a network that joins the observational activities of tens of observers across Europe and the Mediterranean Sea, exceeding 1000 observations per year. In particular, a coordination effort over 2009 through 2013 led to the production of a first database of observations with a broad coverage of regions over Europe and the Mediterranean Sea. The increased number of observations was accompanied by the first detection of extremely rare phenomena such as the first GJ observed over Europe (van der Velde et al. 2010a; Kułak and Młynarczyk 2011; Neubert et al. 2011), detailed analysis of individual sprite-producing thunderstorms (Soula et al. 2014, 2015, 2017), of sprite parent lightning (van der Velde et al. 2014), and elve statistics of a specific region (van der Velde and Montanyà 2016), high-speed recording of sprites (Montanyà et al. 2010), sprites signatures in radio waves (Farges and Blanc 2011; Füllekrug et al. 2013b; Młynarczyk et al. 2015), long-lasting TLE signatures in the ionosphere induced by rare very strong lightning (Haldoupis et al. 2012, 2013). More recent studies included also detailed impact of sprite-producing thunderstorms on the atmosphere above with consequent relativistic acceleration of electrons (Füllekrug et al. 2013a) in association with model studies (Chanrion and Neubert 2010), impact of sprite-producing thunderstorms on the lower ionosphere (especially on the sporadic E layer) over Central European region (Barta et al. 2017) using ionosonde data, or may lead to joint studies also with detection of terrestrial gamma-ray flashes over the Mediterranean Sea (Gjesteland et al. 2015).

1.3 A Climatological Perspective

Such a large number of observations allow for the first time detailed climatological studies to be performed over Europe and the Mediterranean Sea, therefore studying the geographical distribution and variability of mean TLE occurrence over a time span of several

years rather than looking at individual events. A Southern Mediterranean example was presented by Yair et al. (2015), and an introduction to the climatology presented here was published by Arnone et al. (2016). Despite being inhomogeneously distributed, the number of ground-based observed sprites largely exceeds that acquired globally from satellites over equivalent periods of time (Chen et al. 2008). They give therefore an essential contribution to climatological studies, which remain fundamental for understanding the global role of TLEs in the atmosphere (see, for example, reviews by Pasko 2010; Pasko et al. 2011), e.g., answering questions on the spatial and temporal distribution of their occurrence and of their impact; opening the way to comparison with other climatological atmospheric and climate data for which one-to-one analysis is not meaningful; allowing calibration of climatologies based on non-optical measurements, such as through Schumann resonances and detection at extremely low frequency (ELF, Füllekrug and Reising 1998; Whitley et al. 2011). The climatology of TLEs with associated details for individual TLE types and relationship to lightning opens the way to further interpretation in future studies dealing, e.g., the meteorology and the global electric circuit.

A branch of European TLE-related activities that has developed over the past years and will greatly benefit from these large observational samples is that studying the impact of TLEs on the atmosphere. This include model and laboratory studies of the discharges themselves (e.g., Luque and Ebert 2009; Ebert et al. 2010); modelling of their emissions and impact onto the atmosphere and its chemistry at local or global level (Enell et al. 2008; Gordillo-Vázquez 2008; Arnone et al. 2008a, 2014; Gordillo-Vázquez et al. 2011; Parra-Rojas et al. 2013, 2015; Neubert and Chanrion 2013; Winkler and Notholt 2014, 2015; Pérez-Invernón et al. 2018a, 2019); observational studies linking chemistry to TLE occurrence (Arnone et al. 2008c, 2009, 2016; Arnone and Hauchecorne 2012): a number of TLE parametrized distributions have been adopted by several of these modelling and observational studies based on regional to global lightning observations. Furthermore, investigations on the role of sprites in the global electric circuit were also brought forward (Füllekrug et al. 2006; Rycroft et al. 2007; Rycroft and Odzimek 2010; Rycroft and Harrison 2011). More recently, a capability of investigating TLEs with high-resolution spectroscopy was also developed (Gordillo-Vázquez et al. 2018) in association with optical observations of sprites, and methods for the spectroscopic diagnostic of elves and halos were developed for space-based instruments (Pérez-Invernón et al. 2018b).

The growth of this field of research in Europe has brought to the development of the Atmosphere-Space Interaction Monitor (ASIM) that was launched on 2 April 2018, and installed on an external platform of the Columbus Module of the International Space Station. The main objectives of the mission are related to thunderstorm activity by observing associated emissions in the near UV, near-infrared, X-ray and gamma-ray bands. ASIM consists of two main instrument modules, the Modular Multi-spectral Imaging Array (MMIA) with two cameras and three photometers observing in the 180–230 nm, 337 nm and 777.4 nm bands and the Modular X-ray and gamma-ray Sensor (MXGS) observing photons of energy in the range 15 keV to 20 MeV with imaging capability (Neubert 2009; Neubert et al. 2019). A further European mission dedicated to the study of thunderstorms is the TARANIS satellite (Tool for the Analysis of RAdiations from lightNINGs and Sprites) which is planned to be launched in 2020 carrying a set of instruments recording thunderstorm emission in the optical, X-ray, gamma-ray and radio bands (Blanc et al. 2007; Lefeuve et al. 2008). Both space missions will exploit the coordinated ground-based observation systems and the knowledge on TLE distribution and variability discussed in this study.

In this paper, we present the distribution and seasonal cycle of TLE observations from the Eurosprite network and partners during 2009 through 2013, the period with

the widest coverage of European observations to date. The paper aims both at giving an overview of the observational capabilities of the network and exploiting its results to obtain for the first time a climatology of TLEs over Europe. The structure of the paper reflects these aims: the coordinated Eurosprite instrumentation and observations are presented in Sect. 2. The data analysis is described in Sect. 3. The climatology is presented in Sect. 4 and discussed in Sect. 5. Conclusions are given in Sect. 6.

2 Eurosprite Instrumentation

Several partners contribute to the so-called Eurosprite network which provided the observations studied in this work. Eurosprite is an umbrella identifying a coordinated observational effort exploiting several optical cameras permanently installed at strategic locations or temporarily deployed during field campaigns throughout Europe and coastal areas. The main optical systems involved in the network are shown in Fig. 1 with their estimated coverage (see Sect. 3.1). A number of further optical systems contribute with sporadic observations through their regional networks (see below). As shown, most of Central and Southern Europe is well covered by observations, whereas there is as yet limited coverage of Eastern and Northern Europe. The Mediterranean Sea and coastal areas are covered in the Northern parts by systems in Spain, France and Italy, and in the Southern parts by Israel. An overview of the optical systems involved in this study (i.e. active in 2009–2013) and their current status is given here below. An overall description of Eurosprite activities and early campaigns can be found in Neubert et al. (2008).

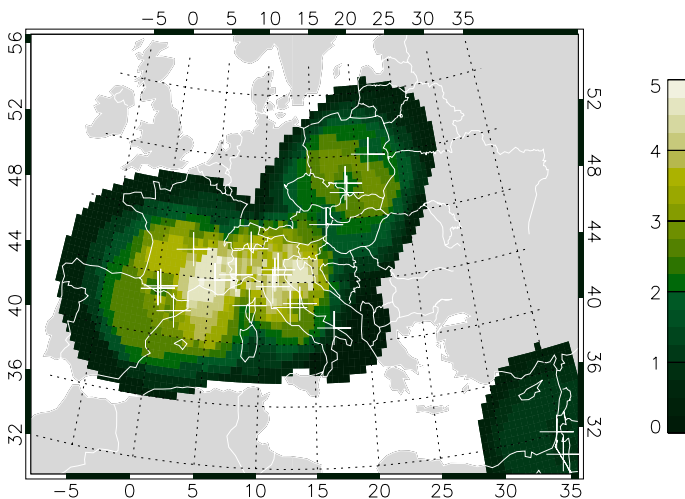


Fig. 1 Location (white crosses) and estimated observational coverage (colour scale) of the main optical camera systems involved in the Eurosprite network. The coverage is reported in terms of number of cameras observing a specific location weighted by the continuity or shortages of the contribution of each camera. See text for details

2.1 Optical Systems

2.1.1 Southern Europe and the Mediterranean Sea

The first operating European sprite-watch system was installed in Southern France at Pic du Midi (42.94°N, 0.14°E, 2877 m) in the French Pyrenees to conduct campaign operations in 2000 and 2003 (Neubert et al. 2001, 2005). It consisted of remotely controlled optical cameras sensitive to low-light conditions and a photometer. This camera system was associated with other similar systems for summer and fall campaigns, especially in 2005 and 2006 with a camera at Puy de Dome (45.77°N, 2.962°E, 1465 m) and in 2008 on Mount Corona (42.46°N, 8.92°E, 2144 m) in Corsica, and at the Calar Alto Observatory (37.22°N, 2.58°E) (Neubert et al. 2005, 2008; Chanrion et al. 2007; Arnone et al. 2008b; Soula et al. 2010). See Fig. 1. A new low-light and high-resolution charge-coupled device (CCD) camera (Watec 902H), mounted on a pan-tilt unit remotely controlled through the Internet, was installed in 2009 at Pic du Midi and continuously operated. It is equipped with a 12 mm f/0.8 lens with a 31° field of view (FOV). The typical maximum range of such a high mountain system is 800 km, so that this system commonly observes TLEs over the southeastern France, the Alps, the western Mediterranean Sea and a large part of Spain (Soula et al. 2010, 2014, 2015, 2017; van der Velde et al. 2010a, 2014). Other similar cameras are located in southern France at lower altitude, in Lannemezan (43.13°N, 0.37°E, 592 m) since 2007, in Clermont-Ferrand (45.76°N, 3.11°E; 400 m) since 2010, in Rustrel (43.94°N, 5.48°E, 1020 m) since 2011. These four cameras can be operated throughout the year. In particular, during the period considered for this study, the Pic du Midi system was active in 2010 (mid-July to end of August), 2011 (mid-May to end of November) and 2013 (mid-August to end of September); the Corsica system in 2009 (August to mid-November), 2010 (mid-July to mid-October) and 2011 (second half of July); the Calar Alto system in 2009 (mid-April to mid-November) and 2011 (end of September to mid-December). In September 2018, a high-speed remote camera system was mounted at the top of the Laboratoire Souterrain à Bas Bruit (LSBB) in Rustrel (43.93°N, 5.49°E) and another system at the Observatoire Midi-Pyrénées is planned for installation in 2019.

Observations taken from Spain were based on a remotely controlled camera installed at Sant Vicenç de Castellet (41.67°N, 1.85°E) and additional deployable cameras including a high-speed system (see Fig. 1). The remotely controlled system has an observation range of about 150–450 km centred on the camera location, with minimum distance rarely below 100 km (about 35° high in the sky) and reaching a maximum distance of about 600 km. The viewing had partial limitation towards Southern France because of hills blocking the lowest 12°. The system was moved to Castellgalí (41.67°N, 1.83°E) in November 2013 where it continues operations. The cameras were operated continuously throughout the year, with observations taken when viewing conditions were clear and manually operated whenever there were storms.

Observations from Italy and Switzerland were recorded by the Italian Meteor and TLE Network (IMTN), which groups over 30 cameras with fixed pointing and a few automated pointing cameras. IMTN fully covers central and Northern Italy, and adjacent regions, and has some limited sensitivity down to Southern Italy. Most cameras are close to sea level and close to cities, so that the observation range of each camera is limited to a few hundred km. Because of multiple cameras covering the same areas from different location, it is often possible to triangulate. The most active stations (i.e. with more cameras and continuity of observations, resulting in more observations taken) are installed at

Ferrara (44.83°N, 11.57°E), Tortoreto (42.66°N, 13.67°E), Contigliano (42.41°N, 12.76°E), Bologna/Medicina (44.50°N, 11.26°E), Lugano/Gnosca (46.12°N, 8.84°E), Cuneo (44.39°N, 7.48°E) and Scandicci (43.74°N, 11.08°E). The southernmost camera is placed in Casamassima (41.03°N, 16.82°E) since 2012. In 2010, a research camera with a remotely controlled automated TLE detection system was mounted at the Italian Climate Observatory on Mount Cimone (44.19°N, 10.70°E, 2165 m), Modena, Italy. The system was moved to the Loiano Observatory (44.39°N, 11.19°E) in early 2013 and continues to be operational. The overall coverage from Italy includes adjacent seas, parts of central Europe and the Balkans (see Fig. 1). The cameras are operated throughout the year. The network of overlapping camera viewing is demonstrated to be extremely efficient in capturing TLEs, leading, for example, to the only GJ captured to date over Europe (van der Velde et al. 2010a). Despite shortages in the viewing conditions and continuity of the operation of individual cameras, these regions can be considered to be largely continuously monitored.

Covering the western Mediterranean Sea and adjacent regions, observations were conducted from Israel by the ILAN (Imaging of Lightning And Nocturnal flashes) team. The TLE observing system is deployed on the rooftop of the Geophysics department of Tel Aviv University and is comprised of two panchromatic CCD cameras, mounted on a remotely controlled pan-and-tilt unit (Ganot et al. 2007) (see Fig. 1). Observations are conducted during the thunderstorm active period of September–May every year, with a line of sight stretching up to Cyprus and Southern Turkey (Yair et al. 2009). For specific storm events, an alternative site at the Wise astronomical observatory (30.60°N, 34.76°E) in the Negev desert was used, extending the coverage to the Nile delta and beyond.

2.1.2 Central Europe

Organized TLE observations in Central Europe started in 2007. An optical detection site has been set up in Sopron, in the North Western part of Hungary (47.69°N, 16.44°E) with a remotely controlled monochrome analogue video camera. Due to the vulnerability of the applied pan-tilt unit, the camera used to be dismantled for the winter and reinstalled in the following year (see Fig. 1). Observations were taken in May to August, June to August, and July to October, in 2009, in 2010, and in 2011, respectively. Further details of TLE-related observations in Hungary can be found in Sători et al. (2013). Recently, another TLE observation site has been set up in southern Hungary at Baja (46.18°N, 19.01°E) with similar instrumentation to that in Sopron, in the North Western part of the country. The new site covers central Italy, the Adriatic Sea, and the middle and the North-Western part of the Balkans.

Observations from Czech Republic started in May 2011 with a camera installed at Nydek (49.67°N, 18.77°E) and continued thereafter all year round with only very minor breaks during the period of this study (5–21 July 2011, 5–26 November 2012 and 1–14 November 2013). See, for example, Mlynarczyk et al. (2015). Observed TLEs occurred between May and November. The contribution from this region reached about 700 TLEs, covering Czech Republic, Slovakia, Germany, Austria, Poland, Hungary, Ukraine and extending to Italy, Slovenia, Croatia and the Adriatic Sea with distances from the observer ranging between 100 and 700 km.

The first TLE research observations in Poland have been carried out during a 2-week field campaign at Mount Sniezka (50.74°N, 15.74°E), the highest peak of the Sudetes, in July 2007 organized as part of EuroSprite (Odzimek et al. 2008; Iwański et al. 2009). Since summer 2011, research observations have also been made sporadically from

Gliwice (50.28°N, 18.65°E) with azimuth 180°–300° and from Swider (52.01°N, 21.39°E) with azimuth 300°–50°. These observations have been carried out using low-light sensitive cameras pointed manually, covering parts of Germany, Austria, Hungary, the Czech Republic and Poland (see Fig. 1), as far as Southern Lithuania from Swider. Large parts of this area overlap with those covered by systems in Hungary and the Czech Republic, therefore allowing triangulation. It has also to be noted that tens of sprites each year have been observed from Poland since 2009 by the Polish Fireball Network (PFN). PFN operates cameras at fixed direction over the territory of Poland with stations disseminated over central, North West, and South West Poland, and two stations in the East, with limited and variable viewing directions for all stations. PFN stations with the longest detection period or the most of the observed events are Gniewowo (54.58 N, 18.30 E) which made the first PFN detection in 2009, Twardogora (51.37 N, 17.46 E), Nowe Miasto Lubawskie (53.43 N, 19.59 E), Blonie (52.19 N, 20.62 E) and Chelm (51.16 N, 23.50 E).

2.1.3 Northern Europe

Optical observations of TLEs in Northern Europe have to deal with the basic problem that the sky is seldom dark during summer, when most Northern European thunderstorms occur. A station has been operated at Esrange, Kiruna, to look for sprites over winter thunderstorms over the Atlantic coast of Norway. In Finland, there is an extensive network of amateur astronomers and storm chasers related to the Astronomical Association Ursa running automatic detection software for observing bolides and other bright events in the twilight and night sky. In 2009, the northernmost European sprite and elve were recorded (Mäkelä et al. 2010). In 2009–2013, a total of 25 TLEs were observed (24 sprites, 1 blue jet).

2.2 Lightning Detection

Lightning detections from national networks were used both as guidance for pointing direction during the observations and in order to geolocate the TLEs with their parent lightning in post-processing of TLE data. In particular, lightning data came from the VLF/LF radio lightning detection network (LINET, Betz et al. 2009) network in Italy, Spain, Hungary, Poland and Germany. Data from Meteorage and from the European Cooperation for Lightning Detection (EUCLID) were adopted in France and nearby areas. Lightning data from the community lightning detection network BlitzOrtung were used by automated pointing cameras in Italy and Czech Republic. In Poland, lightning detection was acquired also from the Institute of Meteorology and Water Management lightning network (PERUN) and Central Lightning Detection Network (CELDN). In Finland, the lightning location data are from the Nordic Lightning Information Systems (NORDLIS, Mäkelä et al. 2010). Additionally, satellite infrared images and local radar images are used for both pointing and data geolocation.

The analysis of lightning over Europe was performed adopting data from the World Wide Lightning Location Network (WWLLN). Detection of lightning in WWLLN is based on the consistent recording of VLF band spheric signals from lightning strokes at five stations (as a minimum) of the network. WWLLN processes the signals from its receivers centrally and uses the time-of-arrival method to calculate geographical location and the time of occurrence of the source of the detected signals with 10 km and microsecond average accuracy, respectively (Rodger et al. 2006; Rudlosky and Shea 2013). Since 2009,

WWLLN detectors covering continental Europe and the Mediterranean Sea are placed in Portugal, Hungary, Israel and Northern Finland, whereas a new detector was activated in 2012 in the UK. The switch on of the UK detector may lead to an increase in the detection rate since 2012.

We note that the detection efficiency in the WWLLN system is low for individual lightning strokes when compared to local or regional lightning detection networks (Abarca et al. 2010). This limitation, however, corresponds to weak discharges. The overall detection efficiency ranges between 15 and 30% depending on geographical location, biased towards strong lightning. It is known that the appearance of sprites is predominantly triggered by intense + CG lightning (e.g., Neubert et al. 2008) and that sprite halos and elves are produced by high-peak-current lightning strokes (Williams et al. 2012; van der Velde and Montanyà 2016). Unfortunately, WWLLN does not report peak currents nor the type (cloud-to-ground/inter-cloud, CG/IC) of the stroke, so its full lightning database, as it is considered in this study, contains many lightning strokes which cannot be associated with TLEs. Nevertheless, the good homogeneity of the dataset in 2009–2013 over Europe and the Mediterranean Sea enables it to be used for comparison with TLE observations as an aid in the interpretation of the findings.

3 Observations and Data Analysis

Over 2009–2013, thousands of observations were recorded by the network described in the previous section. Since the range of view of TLEs for these low-light cameras can reach several hundreds of kilometres, TLEs were recorded over large parts of Europe and the Mediterranean Sea, through the complex coverage discussed in the following section. All observations are made of optical images, consisting of one or two consecutive video frames capturing one or more TLEs and one or more elements of a sprite or sprite groups, if present. Given the large number of observations, a very vast family of different types of sprites was registered, including carrot, angel and column sprites, with a variety of shapes and at all levels of detail. Because of detection difficulties, a much lower level of detail characterizes the elve and halo images. The details of TLE images were not analysed in this work favouring the overall climatological aspects of the distribution through the construction of a database (Sect. 3.2) and binning (Sect. 3.3) of the observations.

3.1 Observational Coverage

Figure 1 shows the location of the most representative optical systems that contributed with observations during 2009–2013 (white crosses) with an estimate of their viewing coverage (coloured areas). A main issue with ground-based optical TLE observations is the unevenness of the distribution of the cameras and the continuous changes of their viewing due to either atmospheric processes or experimental changes. Although the main observation hot spots are known (i.e. the areas covered by cameras capturing most TLEs), the detection efficiency is affected in a way that is not possible to characterize correctly for the largest part of the available data, for which detailed historical conditions (e.g., viewing conditions, pointing direction, operating period, observational choice of the observer when more thunderstorms are in view) were not recorded. In order to take into consideration these shortages and avoid introducing analysis biases between different cameras, we adopted and brought forward two approaches in parallel.

Firstly, an approximate coverage was evaluated adopting the same discretization as for the data analysis (0.5°, see Sect. 3.3) and based on the viewing of the most representative camera systems (as introduced above). These systems were selected as main systems of each contributing research group or regional network and on the basis of the continuity of their operations, area covered (e.g., if covering areas that no other cameras are reaching), and reported number of TLEs. Each of these cameras was characterized by a circular area of coverage around its location, with a radius of 300 km (e.g., in a city) to 800 km (e.g., on a high mountain) depending on the geographical location and characterization by the observer. As a first approximation, a circular area was assumed for all cameras with no consideration of their actual viewing direction, assigning a score of 1 to each geographical bin within the circular area of a camera. The score was lowered to 0.5 in the closest 100 km range of the camera (where the high zenith angle may prevent observing TLEs) and in the furthest 100 km ring (200 km for high mountain sites) (because of the expected drop in detection efficiency due to great distances). A weight ranging 0–1 was then applied to the scores of each camera depending on the continuity of operations: fraction of the 5 years 2009–2013 and fraction of individual year (season). By this characterization, a bin within the viewing range of a camera operated throughout the year would get a score 1 if operated during the whole 5 years and 0.8 if operated during 4 years only. The weight was tuned also depending on known shortages or high efficiency of the camera system (from + 0.2 for the most advanced to – 0.2 for novel observers, and assigning a default 1 for the main multi-camera systems at Mt Corona, S.V. Castellet, Ferrara and Teramo). The coverage distribution was then calculated integrating the contributions from all cameras, resulting in maximum scores of 5 (i.e. 5 overlapping cameras) indicating the highest probability of detecting TLEs. The resulting distribution reported in Fig. 1 shows the large areas covered and highlights the areas with higher expected observing capability. This coverage was used to interpret the TLE climatology and to simulate the expected TLE distribution based on the lightning distribution. With this approach, the actual detection efficiency of individual cameras remains to be evaluated a posteriori but can be assumed to be partly compensated and similar among all cameras so that the overall geographical distribution can be correctly interpreted.

Secondly, in order to remove the bias produced by the uneven detection efficiency, we studied seasonal changes of the geographical distribution of TLEs in terms of multi-year seasonal averages normalized by the multi-year yearly average (see Sect. 4.2). We also considered monthly averages integrated over the area where most of TLEs were observed (see white contours in Fig. 3), excluding data from the Eastern Mediterranean Sea in order to obtain a more homogeneous sample.

3.2 The Eurosprite Database

The Eurosprite data used in this study include all available 2009–2013 optical images from the broad network of instrumentation described in the previous section. Individual TLE images were collected by the observers into data entries for the Eurosprite database. Each entry consists of the number of TLEs associated with an individual thunderstorm or closely related thunderstorm cells; the geographical area covered by those TLEs; the period of TLE activity; and the TLE type. TLEs recorded in one individual observation (e.g., several sprite elements in one video frame) were typically counted as one, unless they were clearly discernible as separate events. The geographical coverage of the TLEs was estimated by the observers on the basis of the camera field of view, its pointing direction and correlative

meteorological data. The geolocation was performed either associating the TLE with its parent lightning stroke obtained through lightning detection networks, whenever possible, or with its parent thunderstorm through the overall lightning and cloud conditions in the region of interest. In the database, the TLE data coverage was reported with a $\pm 1^\circ$ latitude and longitude uncertainty for most observations, whereas the timing with a ± 1 min uncertainty. The $\pm 1^\circ$ uncertainty reflects both the inaccuracy of the actual spatial extent of small events, and on their geolocation. Observations reported with higher accuracy were rounded to the closest 0.5° , assuming a minimum spatial extent of 1° . An extract of the database with a selection of the most prolific thunderstorms is reported in Table 1. The database with the complete list of observations was made publicly available (Arnone et al. 2019).

Table 1 Summary of the 30 most prolific TLE-thunderstorms observed in 2009–2013

Date	Time (UT)	Latitude ($^\circ$)	Longitude ($^\circ$)	TLE	Sprite	Elve	Halo
29.10.2013	17:48/5:32	39.0/40.5	3.0/7.5	195	193	0	2
10.06.2009	21:00/2:00	45.0/47.0	19.0/23.0	147	146	0	1
28.11.2011	18:26/2:48	37.0/40.0	3.0/7.0	140	131	8	1
30.08.2012	21:23/4:05	37.0/40.0	0.0/2.5	129	123	0	6
26.07.2013	20:28/2:23	44.0/44.5	- 1.0/1.5	111	111	0	7
12.10.2012	20:15/4:40	38.0/41.0	1.0/4.5	107	98	4	5
06.08.2013	19:37/0:49	48.0/50.0	12.5/14.5	101	84	0	16
28.11.2012	16:39/4:02	40.0/44.0	15.0/17.0	79	79	0	0
30.11.2009	23:14/6:07	38.0/40.0	4.0/6.0	79	14	65	0
29.01.2012	21:18/6:8	36.5/39.0	0.0/5.0	78	18	59	4
08.10.2009	18:17/0:47	43.0/44.0	2.0/5.0	77	77	0	2
12.11.2011	22:19/23:01	33.0/35.0	31.0/33.0	75	75	0	0
27.05.2009	21:10/2:18	42.0/46.0	12.0/16.0	69	69	0	0
20.08.2012	20:26/2:37	46.5/49.5	9.0/14.5	62	61	0	1
22.11.2013	1:31/5:54	41.0/42.5	4.0/8.0	62	10	50	2
25.12.2013	21:34/6:21	43.5/47.0	- 7.0/- 1.0	61	14	47	5
09.11.2010	19:59/5:30	43.5/44.5	- 5.5/- 0.5	58	1	57	0
02.07.2012	20:15/1:32	49.5/52.0	12.0/16.5	54	51	0	4
12.12.2009	22:26/3:05	41.0/42.0	6.0/7.0	54	47	2	3
20.06.2013	21:26/1:14	50.5/54.0	11.0/16.5	53	53	0	0
02.08.2009	21:15/1:00	49.0/51.0	15.0/19.0	52	52	0	0
09.01.2012	0:26/5:30	41.5/43.5	14.0/16.0	50	50	0	0
24.09.2012	17:47/22:24	45.0/47.5	12.5/18.0	50	50	0	0
02.07.2012	20:09/1:32	50.5/51.5	14.0/15.5	50	49	0	0
24.11.2013	18:55/5:31	39.0/41.0	6.5/7.5	49	8	39	4
28.11.2010	19:31/3:45	43.5/45.0	- 6.0/- 1.0	49	0	49	0
06.11.2011	18:01/23:25	42.0/44.0	13.0/16.0	46	2	0	0
25.01.2010	22:00/22:00	35.0/37.0	- 3.0/0.0	44	40	4	0
20.06.2013	20:38/0:43	51.5/53.0	14.0/15.0	43	38	0	5
20.08.2012	19:18/3:04	47.0/49.0	9.5/13.5	42	42	0	0

3.3 Binning of Observations

In order to avoid being affected by uncertainties on individual events, we studied the observed TLEs only in terms of climatology, i.e. their mean distribution and variability. Eurosprite data entries were binned over 0.5° latitude and longitude bins, and over 1-month intervals, distributing their contribution among all bins affected by the data entry/thunderstorm area. This implies that an oversampling and smoothing was performed of data over a grid finer than the given uncertainty, in order to obtain an increased resolution allowed by higher accuracy observations and overlap of several observations. Overlapping observations of the same events by multiple cameras was either accounted for directly by the observers (this is the case of, for example, the several cameras of the IMTN network), or by removal of the database entry with less counts in the case of entries that clearly overlap in space and time. The latter removal was applied only to cases reporting more than 20 TLEs to avoid rejecting cases where few different TLEs were captured by different cameras over the same region. Seasonal and yearly averages were calculated based on monthly means.

Lightning data from the WWLLN network were also analysed in a similar fashion, producing a climatology with number of detected strokes within individual geographical bins in a certain season or year. In addition to that, the subset of lightning strokes which occurred during the night was considered separately. Nighttime strokes were selected by considering the time of the local sunset and sunrise. For lightning climatologies, we adopted a discretization of 1° in latitude and longitude in order to be less affected by differences at too fine regional scale and allow an easier interpretation of the TLE distribution main features. In several occasions, we studied lightning data within the limited area of camera coverage or that delimiting the actual TLE observations (see further details below) and performed integration of the overall stroke counts over these regions to obtain monthly means. WWLLN lightning climatologies were used also to evaluate the distribution of TLE-to-stroke ratio and to simulate the expected TLE distribution based on detected strokes. In these calculations, the size of bins of the TLE climatology was accordingly increased to 1° .

4 Results

4.1 Eurosprite Observations in 2009–2013: TLE and Lightning Climatologies

In the years 2009–2013, Eurosprite and partners recorded 8394 TLEs over 1018 thunderstorms. The vast majority of observations were sprites, with 7157 classified events, followed by 641 elves and 280 halos. Also observed were 70 upward lightning processes, 2 blue jets and the first European gigantic jet (the latter recorded in December 2009, west of Corsica—see further details in van der Velde et al. 2010a). The remaining fraction of the events (4%) were reported as unclassified TLEs.

The climatology of TLEs above Europe and Southern Mediterranean Sea for 2009–2013 is reported in Fig. 2 as density of observed TLEs ($\text{TLEs} \times 10^{-3} \text{ km}^{-2} \text{ year}^{-1}$). All TLE types were merged into the climatology to allow an overall view of the activity of TLE-producing thunderstorms above Europe. The figure reports also individual climatologies for the three types of TLEs giving the largest contributions to the database, i.e. sprites, elves and halos. In a similar way, the 2009–2013 climatologies of WWLLN lightning strokes as total daily counts and nighttime only counts are reported in Fig. 3 ($\text{strokes km}^{-2} \text{ year}^{-1}$). Since TLEs are observed only during nighttime, the latter should be preferred for comparison, although

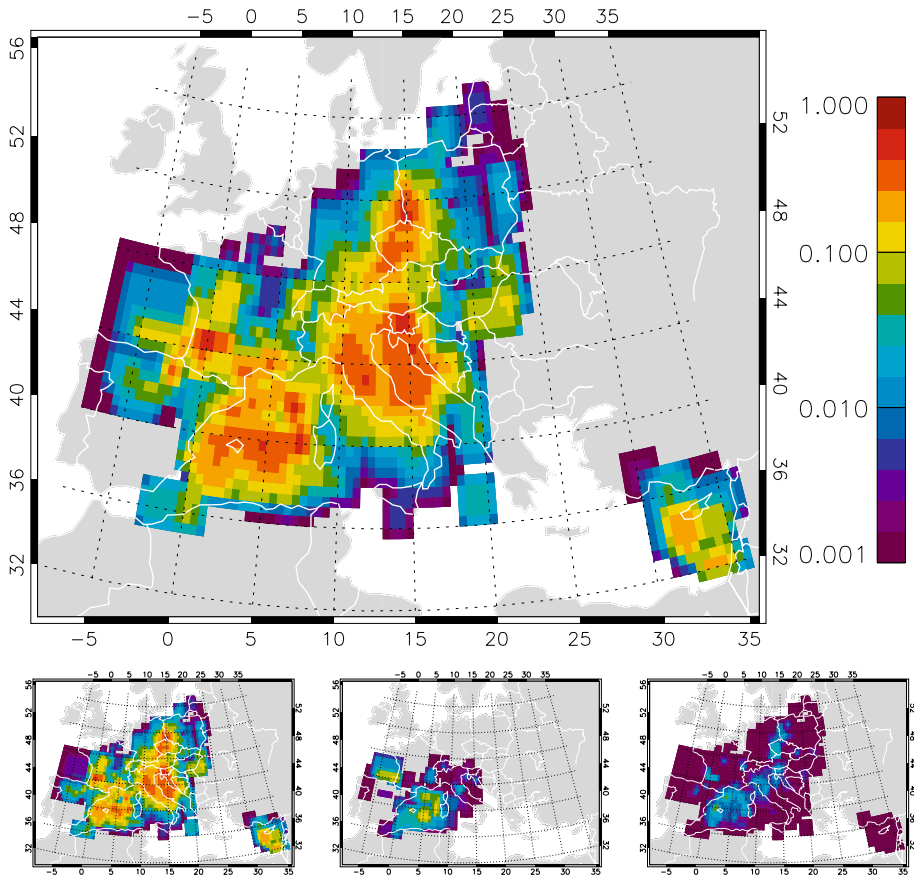


Fig. 2 Top: climatology of observed TLEs ($\text{TLEs} \times 10^{-3} \text{ km}^{-2} \text{ year}^{-1}$) for 2009–2013. Bottom: climatology of observed sprites, elves and halos (left to right). All panels adopt the same colour scale

both maps show relevant information on the geographical distribution of thunderstorm activity over Europe and the Mediterranean Sea. In particular, total lightning can be more correctly compared to climate parameters in terms of, for example, temperature, winds and precipitation. To ease comparison, the main area of observed TLEs over Europe is reported in the WWLLN map as reference (see white contours).

The geographical extension of TLE activity closely resembles the estimated observational coverage, therefore supporting the overall viewing range adopted for the cameras. Drops in recorded TLE rates can promptly be associated with decreases in observational coverage. High TLE activity is found in Southern France and around the Balearic Islands, in Italy and adjacent seas, then extending over Austria and the Czech Republic to the North, towards Hungary to the East, and with a separate set of observations around Cyprus. Despite the biases introduced by the location of the observational systems, some main features in the observed TLE climatology can be extracted with consideration of both observational coverage and lightning activity. Within the regions covered by the observations, the TLE main geographical distribution tends to mimic the distribution of thunderstorm activity. This is evident in the northern part of the TLE climatology where large areas with

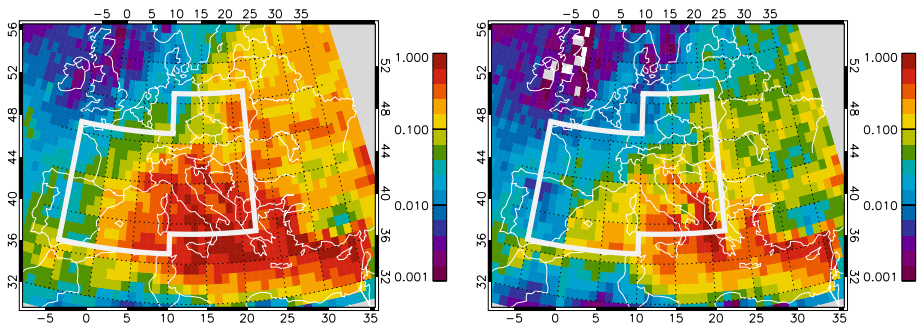


Fig. 3 Climatology of lightning strokes detected by WWLN (strokes $\text{km}^{-2} \text{year}^{-1}$) for 2009–2013 considering the whole day (left) and nighttime only (right) counts. The white thick contours delimit the approximate area of TLE observations used in monthly mean calculations of WWLN data

a weak TLE rate are consistent with a drop in lightning activity over vast areas, e.g., in France and Germany, and particularly over Spain contrasting with the adjacent high activity over the Pyrenees. Interestingly, some local drops in TLE rates are consistently seen in lightning, as, e.g., over Eastern Italy, and likely Sardinia, a behaviour that is related to nighttime lightning and less evidently to total lightning. Further similarities occur in the coastal areas of Northern Spain and Western France, where increased TLE rates are correlated with weakly increased nighttime lightning rates (more visible with a dedicated change of the colour scale here not shown) and more evident in total lightning. High TLE rates are recorded at the German–Polish border with partial correlation to lightning activity (see spots of high lightning activity in this region more visible in total lightning), whereas the high activity over Czech Republic is not reproduced by a similar increase in strokes counts. In contrast, the fading of TLE activity in Southern Italy and towards Eastern Europe is due to poor coverage. The poor coverage causes similar low rates over Corsica, North West Italy and Hungary, where local cameras tend to observe only thunderstorms that occur at a certain distance from the observation spot.

As also evident looking at absolute numbers, sprites dominate the TLE climatology. The dominant role of sprites in our observations is also visible in the maps of individual types of TLEs. The TLE climatology closely resembles that of sprites. On the contrary, elves are predominantly observed over sea and coastal areas where they mostly reinforce features already present in the sprite climatology rather than changing it substantially. The only large change is over the Atlantic Ocean North of Spain where almost no sprites were detected. Halos are observed both over sea and land, again not showing any peculiar features not seen in the sprite climatology. The observation of elves and halos are affected by the much lower detection efficiency found in low-light ground cameras as compared to sprites. Their resulting individual climatologies should be treated with care since they are more sensitive to the different optical system adopted.

4.1.1 TLE Occurrence Rate and TLE-to-Lightning Ratio

The peak TLE occurrence rate is close to or exceeds $10^{-3} \text{ km}^{-2} \text{ year}^{-1}$ in a few hotspots in Southern France, Northern Mediterranean Sea, Italy, the Balkans and the German–Polish border, whereas it is typically around $0.2\text{--}0.3 \times 10^{-3} \text{ km}^{-2} \text{ year}^{-1}$ in large adjacent regions.

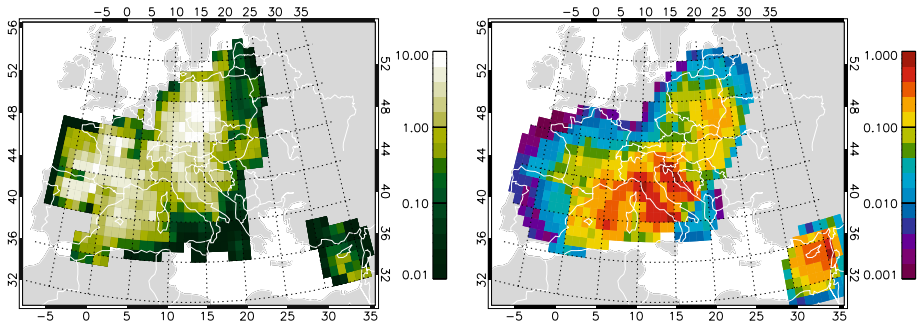


Fig. 4 Left—ratio of observed TLEs to 10^3 WWLLN nighttime strokes for 2009–2013. Right—expected TLEs based on WWLLN nighttime strokes (see Fig. 3), observational coverage (see Fig. 1) and an average 4/1000 TLE-to-nighttime stroke ratio (see left panel)

These rates and the main features of the climatology should be largely assigned to sprites, since the other observed TLEs represent a minor fraction of the database. Elves were mostly observed over autumn/winter maritime thunderstorms in the Northern Mediterranean area, reaching rates in the order of $0.02\text{--}0.2 \times 10^{-3} \text{ km}^{-2} \text{ year}^{-1}$. Halos peaked at $0.02 \times 10^{-3} \text{ km}^{-2} \text{ year}^{-1}$ in most active regions. Comparison to total lightning rates seen in the lightning climatologies of around $0.2\text{--}0.3 \text{ km}^{-2} \text{ year}^{-1}$ within the same regions (see Fig. 3, left) suggests a factor around 1/1000 in the ratio of observed TLE to detected total lightning on a yearly average (recall the factor 10^{-3} in the TLE climatologies). To further inspect this relationship, the TLE-to-nighttime lightning stroke ratio is shown in Fig. 4 and was evaluated adopting a lower resolution 1° climatology of TLEs. Typical values of the ratio are of the order 1–10 in regions well covered by observations and exceed 10 in a few hot spots previously identified, particularly in the area around the German–Polish border where many more TLE per lightning stroke are observed. This ratio greatly changes as a function of season, with average values over the reference region of 0.5/1000 in February, 3/1000 in July and 1.5/1000 in November. (The seasonal cycle will be discussed in Sect. 4.2.)

Taking into consideration the shortages in the observational coverage, we can evaluate an average TLE-to-lightning stroke ratio only on those bins which have the highest ratio values. When considering the bins with the top 50% of the ratio values, the mean TLE-to-nighttime lightning stroke ratio is 2.7/1000; when considering the top 30%, the mean ratio increases to 4.3/1000 (corresponding to a value of 1.3 when total lightning is used in place of nighttime lightning). Note that over the whole climatology, the rate of nighttime to total lightning has a mean value of 0.39 and median value of 0.37, with higher values over coastal areas and sea, and lower ones over continents (not shown).

4.1.2 Simulated TLE Distribution

Based on the above results, we simulated an expected observed TLE distribution scaling the nighttime lightning climatology (see Fig. 3) by the observational coverage (see Fig. 1) and the estimated TLE-to-nighttime lightning ratio 4/1000. The observational coverage was normalized to a maximum value of 1. The results are shown in Fig. 4, right panel. The simulated TLE distribution now carries information on both lightning distribution and

observational coverage, with maximum values scaled by the adopted TLE-to-lightning ratio. The main characteristics and typical values seen in the observed TLE climatology are found also in the simulated one, e.g., overall extension and shape of the area covered by the observations, main active regions and the overall values, features of the high rate areas and low rate ones. Also, some peculiarities of the observed climatologies can now be more easily interpreted on the base of a simultaneous effect of lightning activity and camera sensitivity. This is the case of the TLE distributions in Northern Spain and Western France (where the line features could be better reproduced with a change in the colour scale—not shown) or the drop in central Spain; high rates in the Southern France coast and close to the Balearic Islands; and drop in the rates over Sardinia. The simulation reproduces correctly the observed drop over coastal Eastern Italy, Northern France and Germany and can also pick out the behaviour of the distribution observed over Hungary. In contrast, the simulation does not replicate the behaviour of the climatology over Czech Republic, Slovakia and Poland, where the observational coverage can be further refined. This can be done possibly in dedicated studies where the actual field of view of each camera is considered. The simulation also predicts higher than observed rates around Cyprus because of the local very intense lightning activity, although the overall area is reproduced suggesting lower weights should be estimated via dedicated studies.

The comparison of the observed and simulated TLE climatologies was evaluated quantitatively by inspecting the probability distribution functions and main statistics of the two datasets, considering a 1.0° lower-resolution TLE climatology which was found not to differ in its statistics from the original 0.5° resolution climatology. The TLE and simulated climatologies have about 530 and 590 points, respectively, with TLE rates greater than zero and lead to very similar probability distribution functions (not shown). Mean TLE rates for the observed climatology are 0.07, 0.10 and 0.21 (medians 0.03, 0.07 and 0.19) $\times 10^{-3} \text{ km}^{-2} \text{ year}^{-1}$ considering only geographical bins with rates above 0, above 0.01 and above $0.1 \times 10^{-3} \text{ km}^{-2} \text{ year}^{-1}$, respectively. In comparison, mean TLE rates for the simulated climatology are 0.11, 0.13 and 0.25 (medians 0.05, 0.07 and 0.20) $\times 10^{-3} \text{ km}^{-2} \text{ year}^{-1}$, respectively. The slightly higher mean values of the simulated climatology can be reduced adopting a TLE to nighttime lightning rate of 3/1000 to 0.08, 0.10 and 0.21 (medians 0.04, 0.06, 0.17) $\times 10^{-3} \text{ km}^{-2} \text{ year}^{-1}$, although at the expense of the median which is also slightly reduced, and of a poorer simulation of rate values over some areas (e.g., Spain and France). Overall, the adoption of a 3.5 or 4/1000 ratio seems to be adequate, supporting a posteriori what was previously calculated based on the top 30% of the geographical bins with highest rates.

4.2 TLE Seasonal Cycle Above Europe: Changes to the Mean Geographical Distribution

Seasonal averages of the geographical distribution of TLEs for individual years 2009–2013 are presented in Fig. 5. Dark grey shades show the overall area of observed TLEs during each year. As for the yearly average, the same seasonal averages are reported also for WWLLN nighttime lightning strokes in Fig. 6. Colour grading refers to Figs. 2 and 3, respectively. In terms of seasonal change, TLE activity over Europe is concentrated over the sea in winter and then moves to the coastal areas in spring substantially fading in intensity, and it increases and spreads over the continent in summer and relocates again over the sea in autumn. This behaviour is very consistent among the 5 years of the sample. The activity in the Southern Mediterranean Sea is consistent with the onset of maritime

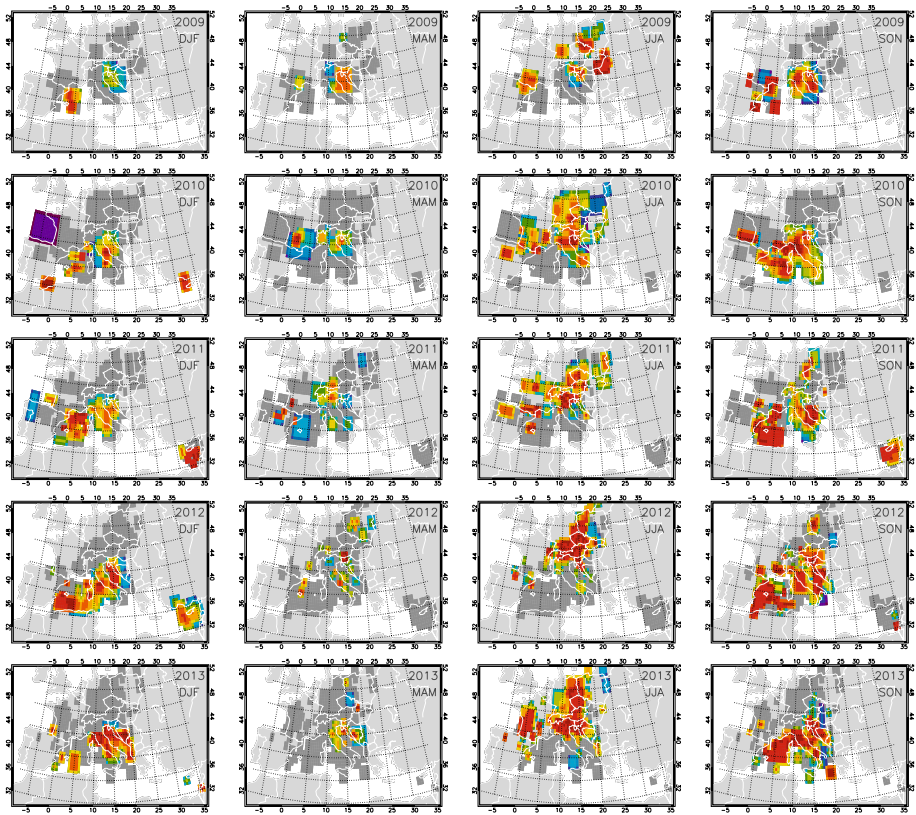


Fig. 5 Climatology of observed TLEs ($\text{TLEs} \times 10^{-3} \text{ km}^{-2} \text{ year}^{-1}$) for individual years 2009–2013 (top–bottom) and season winter (DJF: December, January, February), spring (MAM), summer (JJA) and autumn (SON) (left to right). The area of data coverage of each individual year is shaded in dark grey. Colour grading refers to colour bar in Fig. 2

thunderstorms in autumn and winter (see Yair et al. 2015 for further details). Comparison with Fig. 6 shows a remarkable consistency. Firstly, the general seasonal oscillation of TLE detection between land and sea is consistent with thunderstorm activity. Secondly, detailed comparison of the hotspots of observed TLEs within a certain season corresponds in most cases to regions having the highest lightning rate (see, for example, the coastal and sea areas close to Southern France, Balearic Sea and Italy), or, vice versa, lack of TLEs corresponds to very low lightning rates (e.g., France and Germany as mentioned above). There are clear deviations from this general winter over-sea and summer-land behaviour, e.g., in the case of autumn thunderstorms observed at the border of Czech Republic, Germany and Poland both in 2011 and 2012, or of the large summer activity observed in 2011 around the Balearic Islands. Consistently, in both cases there are signatures of high lightning activity also in WWLLN data. (Note that the maps show the yearly rate per km^2 , so that rates in individual seasons can largely exceed that calculated over the whole year dataset.)

Especially during its first months, 2009 shows a relatively poorer data coverage as compared to the following years. Despite this difference, the main features in the distribution of

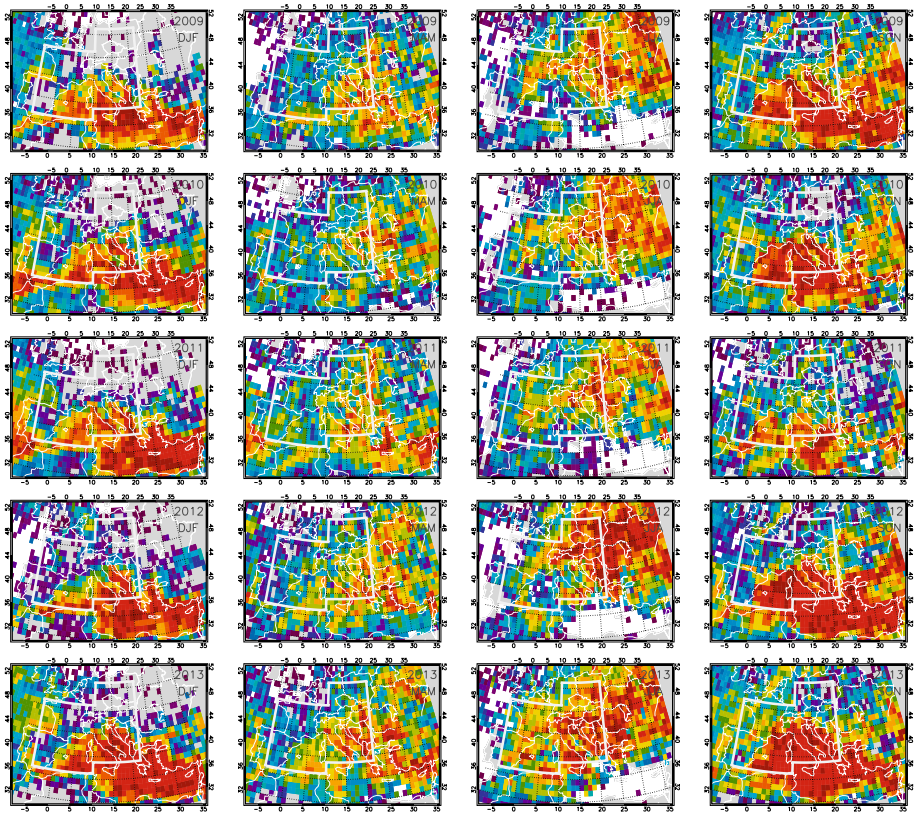


Fig. 6 Climatology of nighttime lightning strokes detected by WWLLN (strokes $\text{km}^{-2} \text{year}^{-1}$) for individual years 2009–2013 (top to bottom) and season winter (DJF: December, January, February), spring (MAM), summer (JJA) and autumn (SON) (left to right). White thick contours of the approximate TLE coverage (Fig. 3) are shown to ease comparison with TLE maps. Colour grading refers to colour bar in Fig. 3

TLEs are repeated over the years, making it meaningful to average the 5 years together as shown in Fig. 2. In order to remove the bias induced by the clustering of optical observation systems over specific regions (see Fig. 1), we normalized the seasonal distributions of the observed TLE activity by the 2009–2013 yearly average (Fig. 2). Results of the normalization are reported in Fig. 7 as per cent component of the yearly mean. The magnitude of the seasonal changes in the distribution of TLEs is now more clearly visible: TLEs are detected largely over the sea in winter followed by a negligible activity over land in spring. In summer, TLEs are detected largely over land and the higher alpine regions (see both activity over the Pyrenees and the Alps) abruptly shifting the activity over the coastal areas and sea in autumn. The strongest activity over the sea in most areas is seen in autumn, together with a strong in activity throughout Italy (with maximum activity spread in autumn and winter). Particularly interesting is the highlight of the activity over the Southern Mediterranean Sea around Cyprus, shifting from the southern area in autumn to the northern area in winter.

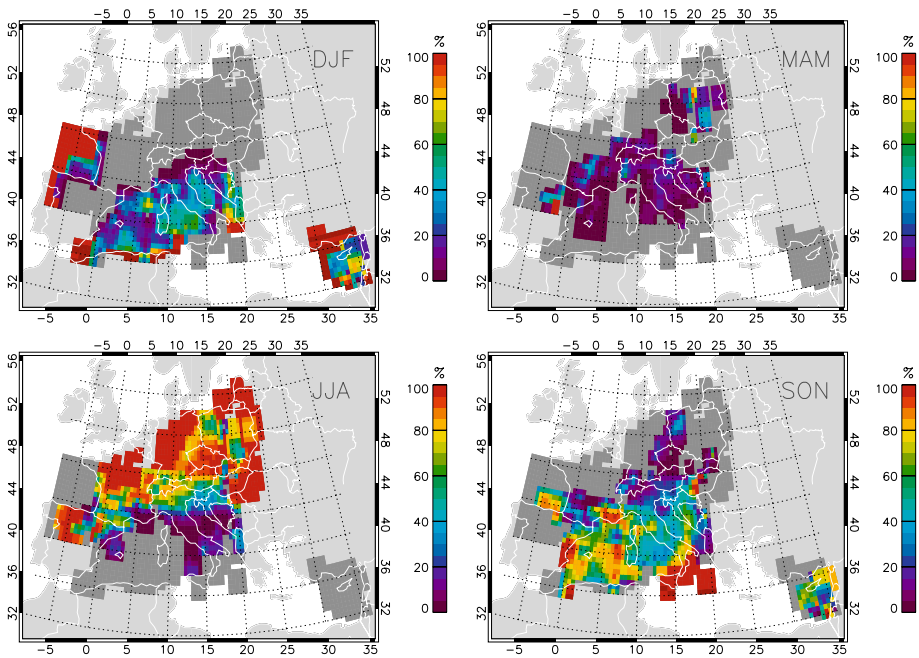


Fig. 7 Average seasonal variation of TLEs (see labels). Data are reported as seasonal fractional component of the 2009–2013 average of Fig. 2. The area of data coverage of the complete data set is shaded in dark grey

4.3 TLE Seasonal Cycle Above Europe: A Monthly Mean Perspective

We further analysed the seasonal evolution of TLEs calculating total average TLE and lightning stroke counts above Europe per month (see Fig. 8). The calculation for TLEs was performed without the inclusion of ILAN observations of the Southern Mediterranean in order to have a more uniform area and a more consistent seasonal behaviour; for consistency, we included only lightning data within the main TLE coverage (see white contours in Fig. 3). Monthly nighttime lightning and TLE counts (Fig. 8) both show a largely consistent seasonal cycle with generally two active seasons (summer and autumn) separated by a deep minimum in late winter–spring (mainly March and April), and a relative minimum in late summer–early autumn (in September for TLEs, and August for lightning but not when including 2013). Maxima are reached in August and November for TLEs, and July and November for lightning. This behaviour is fairly consistent among the 5 years, apart from a very active June in 2009 (which was largely affected by the most prolific thunderstorm in the sample, see Sect. 4.4). Both in summer and autumn, TLEs appear to peak some time later than lightning, but in both cases November is the most prolific month. In Northern Europe, most of the TLE observations are made in late summer (August–October) between 19 and 03 UTC. Despite most of the lightning occurs in June to August in this region, the relative number of TLE detections is lower in this period partly because of the bright summer sky but mostly due to the much higher threshold in lightning charge moment change required to initiate daytime sprites (Stanley et al. 2000).

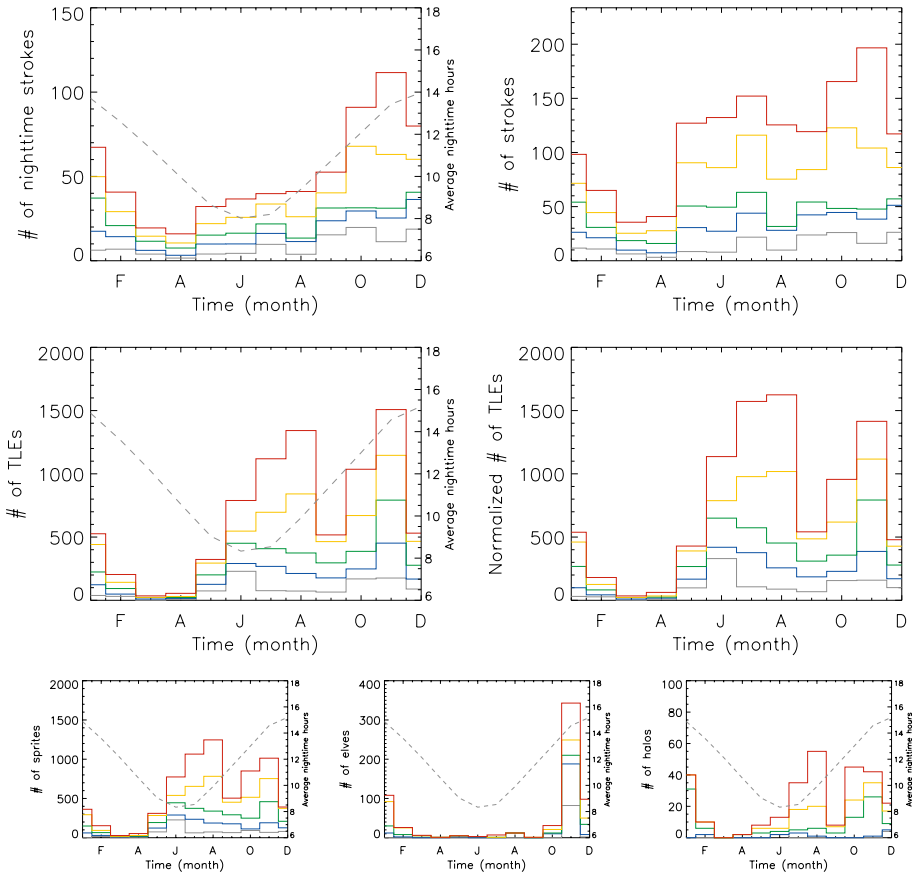


Fig. 8 Cumulative number of observed WWLLN strokes (top), TLEs (centre) and individual TLE types (bottom) per month including data from the start of the sample (January 2009) to the end of 2009, 2010, 2011, 2012 and 2013 (respectively, in grey, blue, green, yellow and red). Lightning is shown in terms of nighttime strokes only (left) and whole day strokes (right). Total TLEs are shown as observed (left) and normalized to a constant 12-h nighttime (right). The adopted average seasonal cycle of nighttime hours is shown in dashed grey. WWLLN data are scaled by a factor 10^4 and averages calculated over the rectangular shapes shown in Fig. 3. Note the change in scale for individual TLEs in bottom panels

In addition to total TLE counts, bottom panels in Fig. 8 report the individual seasonal evolution of the occurrence of sprites, elves and halos (left to right). The overall behaviour of the TLE seasonal cycle is very close to that of sprites, although elves contribute significantly to the November peak, which in the sprite cycle is smaller than the August one. Elves partially contribute also to December and January, making the period November–January the only one with significant activity, consistently with the shift in activity over the sea shown in Fig. 7. Halos tend to mimic the sprite seasonal cycle and lead to no significant effect on the TLE seasonal cycle.

The seasonal evolution of the number of nighttime hours should be taken in consideration when comparing summer and autumn counts since optical observations of TLEs are only available at night. This effect can be very pronounced at high latitude. In order to compensate for the varying length of nighttime conditions, we calculated an average

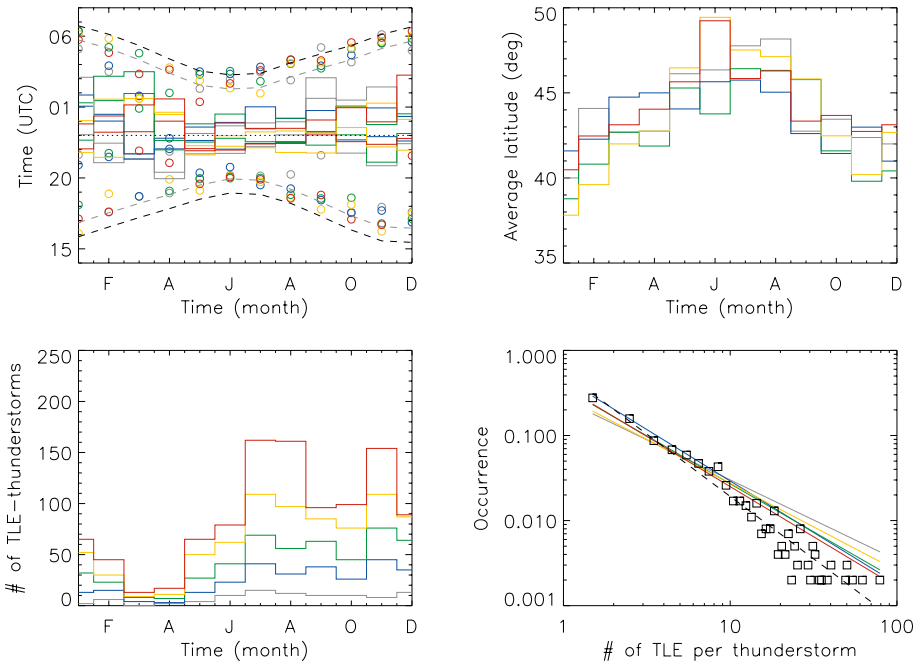


Fig. 9 Top panels show the seasonal evolution of the average time (left) and latitude (right) for 2009, 2010, 2011, 2012 and 2013 (respectively, in grey, blue, green, yellow and red). Time is shown as average start and average end of observations (step lines) and first and last observations (circles) of each month. Dashed lines show the seasonal evolution of the average sunrise and sunset (dark grey), and of an indicative 1 h twilight (light grey). Bottom panels show the cumulative number of TLE-producing thunderstorms per month (left, colour grading corresponds to Fig. 8) and the distribution of the number of TLEs per thunderstorms (right). A power law fit with correlation coefficient -0.96 is shown (dashed black line), together with power law fits for individual years 2009–2013 (colours as in top panels)

nighttime duration (considering duration for Bari, Budapest, Warsaw and Granada—see dashed grey curve in Fig. 8) and normalized the monthly counts to a constant 12-h night. The results are reported in Fig. 8 together with monthly mean lightning activity from the whole day (right panels). The overall TLE behaviour is confirmed, with two distinct summer and autumn seasons now reaching similar total counts per month. An almost flat distribution between May to November is found for lightning, with an increase during July in some years.

An analysis of the time of occurrence of the observed TLEs is shown in Fig. 9 (top-left panel), reporting for each month both the average start and end of the observations (step lines) and the earliest as well as latest observation (circles). The average start and end tends to be very close to the reference local midnight (at 11 UTC, dotted black line) in May to August, then increasing the average observation interval with increasing nighttime hours in autumn and winter, with a tendency to last longer during the second part of the night. First observations of each month generally start 1 or 2 h after sunset (see bottom of the figure), whereas the last observations typically occur within 1 h before sunrise, and sunrise (or slightly beyond). This indicates well that nighttime ionospheric conditions change locally only about 20 min past the ground-level sunrise time (Sátori et al. 2007). Note that the time information for February to April is based on a very limited number of observations.

Figure 9 also reports the seasonal evolution of the average latitude of the observations during the 5 years (top-right panel, compare to Fig. 7). The seasonal changes in the distribution discussed above are now summarized by an average latitude: it cycles between 41° to 42° latitude in autumn and winter and 46° to 47° latitude in summer, with a fairly consistent behaviour among the years, therefore well characterizing the geographical change above Europe. Since the main seasonal change in TLE activity occurs in latitude, no meaningful information can be extracted from average longitude.

4.4 TLE-Producing Thunderstorms

The seasonal evolution of the number of observed TLE-thunderstorms in 2009–2013 is reported in Fig. 9 (bottom-left panel) in a similar fashion as for the number of TLEs in Fig. 8. For consistency, data from Israel were again excluded from the analysis. Here, we assume that each entry of the database (i.e. a collection of TLEs observed above the same thunderstorm or closely related thunderstorm cells) can be considered as an individual thunderstorm system, although some database entries may likely extend over several thunderstorm cells which were observed during the observing period. In general, separated sprite-producing periods were reported so the opposite may also be true: several entries may correspond to the same thunderstorm at different stages. Care should thus be taken to interpret these results correctly. Peaks in number of observed TLE-thunderstorms are reached in July, August and November, consistently with lightning activity, with about 150 TLE-thunderstorms accumulating over the 5 years. Comparison to TLE counts in Fig. 8 (top-left panel) shows that November is characterized by fewer but more prolific TLE-thunderstorms as compared to summer months. Out of 1018 observed thunderstorms, 801 (79%) were reported with less than 10 TLEs each, 921 (90%) with less than 20, 97 (10%) with 20 or more, 56 (6%) with more than 30, 34 (3%) with more than 40. The majority of the observations were related to relatively small thunderstorms and small TLE area. An inspection of the size of the reported TLE area showed in fact about 600 entries reported with a 0–10,000 or 10–20,000 km² area, followed by a second group of about 200 entries with a 30–40,000 km² area and the remaining 200 entries with reported larger areas. Considering that also the possible motion of the thunderstorm during the observation affect the area, this is an indication that the TLE-production area was often close to the size of TLEs and of the uncertainty in their geolocation. Clearly, closer analysis of individual thunderstorms will be needed to further assess the actual TLE-production area.

The distribution in number of TLEs observed per thunderstorm is reported in Fig. 9 (bottom-right panel) in a log–log view. The occurrence is defined as the fraction of thunderstorms having a certain number of TLEs; only cases occurring more than once are considered. The distribution of number of thunderstorms as a function of number of TLEs per thunderstorm (n) follows a power law proportional to n^{-k} as shown by a best linear fit in the log–log plot with coefficient $k = -1.5$ (dashed black line) and having a correlation of -0.96 . The power law fits for individual years 2009–2013 are also shown and have correlation coefficients -0.87 , -0.97 , -0.91 , -0.88 and -0.95 , respectively. The linear fits for individual years are similar among them (-0.94 for 2009 and between -1 and -1.2 for the other years), but have a weaker slope as compared to the multi-year average: this is due to the fact that increasing the number of entries, more bins with more than one count enter the curve and these bins are increasing the weight of the fit on the right tail of the distribution. Correlation coefficients and slopes for individual years and for the multi-year

distribution show a consistent power law behaviour, suggesting the law may be expected to apply for large sample of thunderstorms observed over Europe in future years.

The 30 most prolific thunderstorms are summarized in Table 1. In particular, 12 of these thunderstorms were observed during the summer season (or late spring), and 18 during the autumn–winter season. Seven thunderstorms were reported with more than 100 TLEs each, the most prolific one being observed 29 October 2013 with 195 TLEs (193 sprites and 2 halos), followed by a thunderstorm on 10 June 2009 with 147 TLEs (146 sprites and 1 halo, a thunderstorm analysed in detail by Bór 2013) and by a thunderstorm on 28 November 2011 with 140 TLEs (131 sprites, 8 elves and 1 halo). The 29 October 2013 case was studied by Soula et al. (2017), with more than 100 sprite videos reported in terms of sprite/stroke pairs. The 10 June 2009 thunderstorm makes up most of the anomalously high June TLE count found in 2009 as shown in Fig. 8 (top-left panel). Most of the prolific thunderstorms were reported with almost only sprites. Seven thunderstorms were reported with a significant (greater than 30) number of elves and were all observed during the autumn–winter season (4 in November, one in December and one in January). The 12 December 2009 thunderstorms included observation of the gigantic jet discussed above, and of an upward lightning. For comparison, data for the 12 November 2011 thunderstorm observed from Israel were included in the table: this is the only case of a very prolific thunderstorm observed to last only 40 min, whereas all other prolific thunderstorms observed above Europe and coastal areas lasted several hours each.

5 Discussion

The dataset and climatology presented in the previous section represent the first attempt to have such a coordinated ground-based climatology over Europe and Mediterranean Sea. Similar continuous observations were performed over limited regions such as the US High Plains (Lyons 1996) or in Japan (Adachi et al. 2005; Suzuki et al. 2011). Considering that only a negligible fraction of satellite observations of TLEs are currently taken over Europe (Chen et al. 2008), this is also the largest European TLE dataset available to date. The overall distribution and seasonal cycle of TLEs present robust features repeated in all the 5 years included in the sample, both as number of observed TLE-producing thunderstorms and as number of observed TLEs. This includes the two-peak seasonal cycle, with maxima in summer and late autumn, separated by two minima in March–April and less pronouncedly in September–October. The two active seasons are due to land-driven convection during summer, typically associated with large thunderstorms, and sea-driven convection during autumn and winter, found in synoptic-scale weather systems which transport cold continental air masses over the relatively warm Mediterranean Sea water, leading to instability and convection, and generating smaller thunderstorm cells. For example, the thunderstorm producing 54 TLEs on 12 December 2009, including the first European GJ, was composed by several small cells with cloud top height of only 6 km (van der Velde et al. 2010a). Nevertheless, TLEs were observed to be produced by fewer but more prolific thunderstorms in autumn rather than in summer. The shift of TLE activity from the continental areas in summer to sea and coastal areas in autumn and winter is therefore abrupt both in the region of activity and in the leading processes driving the TLE production.

The observed evolution of the TLE distribution is remarkably consistent with lightning activity reported by the WWLLN network within the region of Eurosprite observations, similarly to the migration from land to coastal and maritime regions previously observed

over the oceans (Füllekrug et al. 2002). The adoption of an observational sensitivity map based on actual regions covered by each camera and the related simulated TLE climatology allows a better interpretation of the main features of the observed climatologies, assigning them to either observational limitations or lightning activity. Considering the number of shortages that were not included in the calculation, the agreement between the observed and simulated climatologies is remarkable. On the one hand, dedicated studies can be planned to further inspect specific regions and try to resolve the differences in terms of observational capabilities. On the other hand, this comparison also sheds light on possible differences in the behaviour of TLE-producing thunderstorms in terms of production rates: can one expect the same TLE to lightning rate for all thunderstorms? Our results point to a very good consistency in the majority of cases but cannot exclude large differences. Discrepancies will therefore need to be further investigated inspecting the + CGs/− CGs ratio or further characteristics of the thunderstorms. Thunderstorm characteristics can be very much different in autumn/winter maritime thunderstorms and in summer continental ones (e.g., McGorman and Rust 1998). Interestingly, our results for the summer season show a very similar distribution as those found with radio measurements by Füllekrug and Reising 1998, their Fig. 3.

This includes also a larger fraction of high charge moment change and high-peak-current lightning, respectively, needed for sprite and elve generation (e.g., Pasko et al. 2011). The climatological approach will aid in the comparison to relevant electrical and atmospheric parameters at large scale.

In agreement with previous studies of European TLE-producing thunderstorms (Neubert et al. 2001, 2005, 2008; Soula et al. 2010; van der Velde et al. 2010b), the majority of TLE-producing thunderstorms in 2009–2013 were relatively small, with a limited TLE area, and were reported to produce a small number of TLEs as compared to large thunderstorm observed, e.g., in North or South America (Lyons 1996; Taylor et al. 2008). The power law we found describing the number of thunderstorms producing a certain number of TLEs is novel and not reported before and would certainly need to be proved also in other continents. This power law behaviour is not unexpected, since it is often found in several other natural phenomena, such as when describing the occurrence and intensity of, for example, tornadoes, fires, earthquakes (see the review by Pinto et al. 2012). Furthermore, it is also found in describing the distribution of terrestrial gamma-ray flashes (TGFs), the second type of exotic emissions produced by thunderstorm activity (Smith et al. 2005). Since the power law was found to be consistent over the 4 most prolific years, it suggests a possible new pathway for modelling the occurrence and distribution of TLEs and TLE-producing thunderstorms above Europe and other regions, so as to further fill the gaps in the observations and allow inclusion in global models (see, for example, the parametrization adopted by Arnone et al. 2014). Given a large sample of TLEs (e.g., from intermittent satellites passages over Europe), the scaling to obtain yearly rates should be performed by clustering the observations over individual thunderstorms as described by the power law. It also allows a new approach for comparing the distribution of TLE-producing thunderstorms over different regions of the globe.

A selection mechanism due to better visibility in winter cannot be excluded to have contributed to observing more elves, halos, upward lightning and blue jets during autumn/winter, besides the expected higher rate of occurrence of elves over the sea. Comparison to Chen et al. (2008) and Newsome and Inan (2010) shows that a strong selection mechanism exists in ground optical observations in favour of sprites: the elve to sprite detection ratio in our climatology is in fact only 1:11 as compared to roughly 6:1 (30:1 accounting for detection efficiency corrections) found by the ISUAL satellite (Chen et al. 2008),

and 6:1 found by ground using high time resolution photometer array (Newsome and Inan 2010). However, the detection of elves almost exclusively over maritime thunderstorms is well in agreement with what found by previous studies (Chen et al. 2008): if limiting to November or January the ratio elves to sprites ratio drops to 1:3. Besides shortages in the optical sensitivity to elves, the algorithms used for identifying elve images in the video frames are also less effective than for sprites. A similar detection bias occurs for halos, which we observed with a 1:26 halo to sprite ratio, whereas in the ISUAL satellite observations it was reported around 4:5. The origin and consequences of different detection efficiency were discussed also by Williams et al. (2012).

As discussed in Sect. 3.1, a key shortage of the adopted dataset is the inhomogeneity of the observational coverage. Cameras have their own detection efficiency, they are often moved to different locations or pointing directions, or their views can be affected by the cloud coverage along their lines of sight. Besides, some cameras are used to track the evolution of thunderstorms (i.e. their pointing direction follows peak activity) and other cameras constantly cover the same region (i.e. they have a fixed pointing direction). The detection efficiency of our network of cameras therefore vary greatly across the observed regions, and this can be even greater when talking about elves and halos which are at the edge of the camera sensitivity. Given the information recorded, an analysis of the detection efficiency of each system was not possible (see, for example, the approach developed by Ignaccolo et al. 2008). The overlap of different cameras can certainly overcome part of the shortages of the individual systems and the adopted sensitivity function was shown to lead to a broad consistency between observed and simulated TLE distributions. Even though one cannot expect a 100% detection efficiency, the observations of the same TLE-producing thunderstorms recorded by multiple cameras of the network suggest a very high efficiency in regions where the coverage function is maximized. The consistency of the observed TLE seasonal changes with the lightning activity shows that the climatological approach is robust if read in terms of TLE-producing thunderstorms. This further underlines the robustness of a joint TLE climatology, considering together TLE-producing thunderstorms, which are often observed to produce several types of TLEs, several of which have likely been missed. This novel climatology therefore represents an ideal reference for several TLE space missions (e.g., GLIMS, ASIM and TARANIS) operating over the next few years. The joint use of ground and space-based observations will improve our simulation and the possibility of extending the climatology outside its current limitations.

6 Conclusions

We presented a first climatology of TLEs over Europe and the Mediterranean Sea based on a coordinated database of optical observations by the Eurosprite ground-based network from 2009 to 2013. The main features of the TLE seasonal cycle were found to be robust, repeating over the years and consistent with lightning activity. The main TLE activity shifts from continental areas in summer to coastal and sea areas in late autumn and early winter. The largest number of TLEs per month is recorded in November, aided by the longer nighttime duration. In March and April, TLE activity is almost completely halted, which, considering the availability of continuously operated cameras and agreement with lightning activity, cannot be due to a bias in active observational campaigns. Elves are observed almost exclusively over autumn–winter maritime thunderstorms, whereas sprites and halos follow the seasonal changes from land to sea.

Taking into consideration both observational coverage and WWLLN lightning activity in a joint simulation, the consistency of the observed TLEs with lightning activity confirms that nighttime lightning is a good proxy for TLEs at large scale. The distribution of nighttime WWLLN lightning can be used to highlight regions where further studies are needed to optimize observational shortages or investigate possible peculiarities in the TLE production. Our analysis points to a 1/1000 (4/1000) TLE-to-(nighttime) lightning ratio. These ratios lead to a TLE global rate of 2.6 TLE min^{-1} (largely a sprite global rate in our case), when they are applied on a global lightning rate of 44 flashes s^{-1} . This value is largely consistent with previous estimates in literature (Ignaccolo et al. 2008). Further consideration of detection efficiency for individual cameras and WWLLN lightning data will need to be adopted to further refine such estimate since the efficiency of both were neglected in our calculation. The same considerations apply to a future refinement of the overall climatology. We also found that given a large sample of TLEs, a power law can well describe how to distribute the expected number of TLE per thunderstorm. These features should be taken into account when investigating the global impact of TLEs onto the atmosphere and parametrizing TLEs into global models. They can also be a valuable guidance for new ground-based observations and current or upcoming space missions.

Despite the consistency on these general features, we found some geographical discrepancies and different rates in some months (e.g., May and September) comparing TLEs to lightning. This confirms that disclosing the details of TLE activity requires further investigation in relation to the type of lightning (e.g., +CG/−CG ratio and intensity) and electrification mechanisms, since of course different types of TLEs are well known to have different production mechanisms. The proposed climatological approach may lead to further advances also in this direction, by comparing large TLE samples to key atmospheric parameters. The very low rate of elve and halo observations is also evidence of the strong limitation of ground-based optical cameras for their observation, stimulating once more a needed synergetic approach with space missions such as ASIM. At the same time, ongoing Eurosprite activities will attempt to remove the main gaps in the observational coverage of Europe and the Mediterranean Sea, for example, including observations from regional all-sky camera networks which have developed over the last years.

Acknowledgements This work was supported within activities of the ESF TEA-IS and ESA-ASIM mission. E.A. acknowledges the support by ESA for the project CHIMTEA within the framework of the Changing Earth Science Network Initiative. Observations of TLEs made by S.S. were partly sponsored by the National Institute of Universe Science (INSU) thanks to LEFE/IMAGO and by the National Centre of Space Studies (CNES). ILAN observations are supported by Israel Science Foundation Grant 117/09, and this research was supported by the Israeli Science Foundation, Grant 145/03. The authors wish to thank the World Wide Lightning Location Network (<http://wwlln.net>), a collaboration among over 50 universities and institutions, for providing the lightning location data used in this paper. The authors are grateful for the essential contributions of all individual observers through their dedication, work on instrumentation and successful observations, particularly to: for IMTN, R. Cabassi, N. Conti, M. Morini, M. Silvestri (CIPH), P. Demaria (Ass. Astrofili Bisalta), L. Barbieri (Ass. Astrofili Bolognesi), M. Mannucci, N. Montigiani (Ass. Astrofili Fiorentini), M. Vivarelli (Gr. Astrofili Montagna Pistoiese), G. Ascione, P. Russo (SkySentinel), S. Eugeni (ANAI), L. Lamacchia (SAIt Puglia), I. Cervini, D. Belfiore, R. Manganelli, T. Maggioni, M. Menichini, M. Morini, F. Palmieri, E. Richetti, A. Severi, S. Sposetti, P. Venturi and all other IMTN node managers; J. Monari (IRA INAF); M. Eltri, E. Stomeo (Unione Astrofili Italiani, Sez. Meteore); D. Cataldi, G. Cataldi (LTPA Observer Project); Z. Andrei (CMN); K. Polakowski, H. Krygiel, J. Laskowski, P. Zareba, J. Baran, M. Maciejewski, T. Krzyzanowski, M. Reszelski (PFN); J. Tóth (Comenius University / SVMN); M. Korošec; R. Spinner. Part of above mentioned networks are now within EDMOND multi-national network. TLE observations at Gliwice, Poland, have been performed voluntarily by M. Mielniczek. The ILAN winter campaigns in Israel were dedicated to the memory of the first Israeli astronaut and sprite observer Col. Ilan Ramon, who died together with the crew of the Space Shuttle Columbia STS-107 on 1 February 2003.

Funding Funding was provided by Hungarian Scientific Research Fund (Grant No. OTKA: K72474), European Cooperation in Science and Technology (Grant No. AP-18: The Physics of Lightning Flash and Its Effects) and European Commission H2020 (Grant No. H2020-MSCA-ITN-2016 no. 722337). Contribution from Hungary was supported by the National Research, Development and Innovation Office, Hungary-NKFIH (K115836). The establishment of the TLE observation site Sopron, Hungary and scientific communication was facilitated by COST Actions P-18, ‘The Physics of Lightning Flash and Its Effects’, and CA15211, ‘ELECTRONET’. The work of MF is supported by the Royal Society (UK) Grant NMG/R1/180252 and the Natural Environment Research Council (UK) under Grants NE/L012669/1 and NE/H024921/1. A.O. acknowledges support from Grants of Poland Ministry of Science and Higher Education to Institute of Geophysics, Polish Academy of Sciences, No. 3841/E-41/S/2018. TLE observations from Swider, Poland, have been supported by earlier Grants Nos. 3841/E-41/S/2012 to 3841/E-41/S/2015. The work of M.P. was supported by the GACR Grant 17-07027S and by the Praemium Academiae award of the CAS.

References

- Abarca SF, Corbosiero KL, Galarneau TJ (2010) An evaluation of the Worldwide Lightning Location Network (WWLLN) using the National Lightning Detection Network (NLDN) as ground truth. *J Geophys Res (Atmos)* 115:D18206. <https://doi.org/10.1029/2009JD013411>
- Adachi T, Fukunishi H, Takahashi Y, Sato M, Ohkubo A, Yamamoto K (2005) Characteristics of thunderstorm systems producing winter sprites in Japan. *J Geophys Res (Atmos)* 110:D11203. <https://doi.org/10.1029/2004JD005012>
- Arnone E, Dinelli B (2016) chap. CHIMTEA—Chemical Impact of Thunderstorms on Earth’s Atmosphere. In: Remote sensing advances for Earth system science, vol. XIII of Springer Earth System Sciences. Springer, Berlin, pp 1–14. https://doi.org/10.1007/978-3-319-16952-1_1
- Arnone E, Hauchecorne A (2012) Stratosphere NO_y Species measured by MIPAS and GOMOS onboard ENVISAT during 2002–2010: influence of plasma processes onto the observed distribution and variability. *Space Sci Rev* 168:315–332. <https://doi.org/10.1007/s11214-011-9861-1>
- Arnone E, Berg P, Arnold NF, Christiansen B, Thejll P (2008a) An estimate of the impact of transient luminous events on the atmospheric temperature. *Adv Geosci* 13:37–43. <https://doi.org/10.5194/adgeo-13-37-2008>
- Arnone E, Berg P, Boberg F, Bór J, Chanrion O, Enell C-F, Ignaccolo M, Mika Á, Odzimek A, van der Velde O, Farges T, Laursen S, Neubert T, Satori G (2008b) The Eurosprite 2005 campaign. In: Arveilius J (ed) Proceedings of the 33rd annual European meeting on Atmospheric Studies by Optical Methods (33AM)
- Arnone E, Kero A, Dinelli BM, Enell C-F, Arnold NF, Papandrea E, Rodger CJ, Carlotti M, Ridolfi M, Turunen E (2008c) Seeking sprite-induced signatures in remotely sensed middle atmosphere NO₂. *Geophys Res Lett* 35:L05807. <https://doi.org/10.1029/2007GL031791>
- Arnone E, Kero A, Enell C-F, Carlotti M, Rodger CJ, Papandrea E, Arnold NF, Dinelli BM, Ridolfi M, Turunen E (2009) Seeking sprite-induced signatures in remotely sensed middle atmosphere NO₂: latitude and time variations. *Plasma Sources Sci Technol* 18:034014. <https://doi.org/10.1088/0963-0252/18/3/034014>
- Arnone E, Smith AK, Enell C-F, Kero A, Dinelli BM (2014) WACCM climate chemistry sensitivity to sprite perturbations. *J Geophys Res (Atmos)* 119:6958–6970. <https://doi.org/10.1002/2013JD020825>
- Arnone E, Bor J, Chanrion O, Barta V, Fullekrug M, Labanti R, Mezuman K, Odzimek A, Popek M, Soula S, Valeri D, van der Velde O, Yair Y, Zanotti F, Zoladek P, Neubert T (2019) The Eurosprite 2009–2013 catalogue (Version 1.3) [DataSet]. <https://doi.org/10.5281/zenodo.3480108>
- Barrington Leigh CP, Inan US, Stanley M (2001) Identification of sprites and elves with intensified video and broadband array photometry. *J Geophys Res* 106:1741–1750
- Barta V, Haldoupis C, Satori G, Buresova D, Chum J, Pozoga M, Berényi KA, Bór J, Popek M, Kis Á, Bencze P (2017) Searching for effects caused by thunderstorms in midlatitude sporadic E layers. *J Atmos Sol-Terr Phys* 161:150–159. <https://doi.org/10.1016/j.jastp.2017.06.006>
- Betz HD, Schmidt K, Laroche P, Blanchet P, Oettinger WP, Defér E, Dziewit Z, Konarski J (2009) LINET—an international lightning detection network in Europe. *Atmos Res* 91:564–573. <https://doi.org/10.1016/j.atmosres.2008.06.012>

- Blanc E, Lefeuvre F, Roussel-Dupré R, Sauvaud JA (2007) TARANIS: a microsatellite project dedicated to the study of impulsive transfers of energy between the Earth atmosphere, the ionosphere, and the magnetosphere. *Adv Space Res* 40:1268–1275. <https://doi.org/10.1016/j.asr.2007.06.037>
- Boeck WL, Vaughan OH Jr, Blakeslee R, Vonnegut B, Brook M (1992) Lightning induced brightening in the airlow layer. *Geophys Res Lett* 19:99–102. <https://doi.org/10.1029/91GL03168>
- Boeck WL, Vaughan OH, Blakeslee RJ, Vonnegut B, Brook M, McKune J (1995) Observations of lightning in the stratosphere. *J Geophys Res* 100:1465–1476. <https://doi.org/10.1029/94JD02432>
- Bór J (2013) Optically perceptible characteristics of sprites observed in Central Europe in 2007–2009. *J Atmos Sol-Terr Phys* 92:151–177. <https://doi.org/10.1016/j.jastp.2012.10.008>
- Bór J, Sántori G, Betz HD (2009) Observation of TLEs in Central Europe from Hungary supported by LINET. In: American Institute of Physics Conference Series, vol 1118 of American Institute of Physics Conference Series, pp 73–83. <https://doi.org/10.1063/1.3137716>
- Bór J, Zelkó Z, Hegedüs T, Jäger Z, Mlynarczyk J, Popek M, Betz HD (2018) On the series of +CG lightning strokes in dancing sprite events. *J Geophys Res (Atmos)* 123:11. <https://doi.org/10.1029/2017J028251>
- Chanrion O, Neubert T (2010) Production of runaway electrons by negative streamer discharges. *J Geophys Res (Space Phys)* 115:A00E32. <https://doi.org/10.1029/2009JA014774>
- Chanrion O, Crosby NB, Arnone E, Boberg F, van der Velde O, Odzimek A, Mika Á, Enell C-F, Berg P, Ignaccolo M, Steiner RJ, Laursen S, Neubert T (2007) The EuroSprite2005 Observational Campaign: an example of training and outreach opportunities for CAL young scientists. *Adv Geosci* 13:3–9
- Chen AB, Kuo C-L, Lee Y-J, Su H-T, Hsu R-R, Chern J-L, Frey HU, Mende SB, Takahashi Y, Fukunishi H, Chang Y-S, Liu T-Y, Lee L-C (2008) Global distributions and occurrence rates of transient luminous events. *J Geophys Res (Space Phys)* 113:A08306. <https://doi.org/10.1029/2008JA013101>
- Cummer SA, Li J, Han F, Lu G, Jaugey N, Lyons WA, Nelson TE (2009) Quantification of the troposphere-to-ionosphere charge transfer in a gigantic jet. *Nat Geosci* 2:617–620. <https://doi.org/10.1038/ngeo0607>
- Ebert U, Montijn C, Briels TMP, Hundsdorfer W, Meulenbroek B, Rocco A, van Veldhuizen EM (2006) The multiscale nature of streamers. *Plasma Sources Sci Technol* 15:118. <https://doi.org/10.1088/0963-0252/15/2/S14>
- Ebert U, Nijdam S, Li C, Luque A, Briels T, van Veldhuizen E (2010) Review of recent results on streamer discharges and discussion of their relevance for sprites and lightning. *J Geophys Res (Space Phys)* 115:A00E43. <https://doi.org/10.1029/2009JA014867>
- Enell C-F, Arnone E, Chanrion O, Adachi T, Verronen PT, Seppälä A, Neubert T, Ulich T, Turunen E, Takahashi Y, Hsu R-R (2008) Parameterisation of the chemical effect of sprites in the middle atmosphere. *Ann Geophys* 26:13–27
- Farges T, Blanc E (2010) Characteristics of infrasound from lightning and sprites near thunderstorm areas. *J Geophys Res (Space Phys)* 115:A00E31. <https://doi.org/10.1029/2009JA014700>
- Farges T, Blanc E (2011) Lightning and TLE electric fields and their impact on the ionosphere. *C R Phys* 12:171–179. <https://doi.org/10.1016/j.crhy.2011.01.013>
- Farges T, Blanc E, Le Pichon A, Neubert T, Allin TH (2005) Identification of infrasound produced by sprites during the Sprite 2003 campaign. *Geophys Res Lett* 32:1813
- Farges T, Blanc E, Tanguy M (2007) Experimental evidence of D region heating by lightning-induced electromagnetic pulses on MF radio links. *J Geophys Res (Space Phys)* 112:A10302. <https://doi.org/10.1029/2007JA012285>
- Franz RC, Nemzek RJ, Winckler JR (1990) Television image of a large upward electrical discharge above a thunderstorm system. *Science* 249:48–51
- Fukunishi H, Takahashi Y, Kubota M, Sakanoi K (1996) Elves: lightning induced transient luminous events in the lower ionosphere. *Geophys Res Lett* 23:2157
- Füllekrug M, Reising SC (1998) Excitation of Earth-ionosphere cavity resonances by sprite-associated lightning flashes. *Geophys Res Lett* 25:4145–4148. <https://doi.org/10.1029/1998GL900133>
- Füllekrug M, Price C, Yair Y, Williams ER (2002) Intense oceanic lightning. *Ann Geophys* 20:133–137. <https://doi.org/10.5194/angeo-20-133-2002>
- Füllekrug M, Mareev EA, Rycroft MJ eds (2006) Sprites, elves and intense lightning discharges, vol. 225 of NATO Science Series II. In: Mathematics, physics and chemistry, Springer, Berlin, ISBN 1-4020-4628-6
- Füllekrug M, Roussel-Dupré R, Symbalisty EMD, Chanrion O, Odzimek A, van der Velde O, Neubert T (2010) Relativistic runaway breakdown in low-frequency radio. *J Geophys Res (Space Phys)* 115:A00E09

- Füllekrug M, Roussel-Dupré R, Symbalisty EMD, Colman JJ, Chanrion O, Soula S, van der Velde O, Odzimek A, Bennett AJ, Pasko VP, Neubert T (2011) Relativistic electron beams above thunderclouds. *Atmos Chem Phys* 11:7747–7754. <https://doi.org/10.5194/acp-11-7747-2011>
- Füllekrug M, Kolmasova I, Santolik O, Farges T, Bór J, Bennett A, Parrot M, Rison W, Zanotti F, Arnone E, Mezentsev A, Lan R, Uhlir L, Harrison G, Soula S, van der Velde O, Pinçon J-L, Helling C, Diver D (2013a) Electron acceleration above thunderclouds. *Environ Res Lett* 8:035027. <https://doi.org/10.1088/1748-9326/8/3/035027>
- Füllekrug M, Mezentsev A, Soula S, Velde O, Farges T (2013b) Sprites in low-frequency radio noise. *Geophys Res Lett* 40:2395–2399. <https://doi.org/10.1002/grl.50408>
- Ganot M, Yair Y, Price C, Ziv B, Sherez Y, Greenberg E, Devir A, Yaniv R (2007) First detection of transient luminous events associated with winter thunderstorms in the eastern Mediterranean. *Geophys Res Lett* 34:L12801. <https://doi.org/10.1029/2007GL029258>
- Gjesteland T, Østgaard N, Laviola S, Miglietta MM, Arnone E, Marisaldi M, Fuschino F, Collier AB, Fabró F, Montanya J (2015) Observation of intrinsically bright terrestrial gamma ray flashes from the Mediterranean basin. *J Geophys Res (Atmos)* 120:12. <https://doi.org/10.1002/2015JD023704>
- Gordillo-Vázquez FJ (2008) Air plasma kinetics under the influence of sprites. *J Phys D Appl Phys* 41:234016. <https://doi.org/10.1088/0022-3727/41/23/234016>
- Gordillo-Vázquez FJ, Luque A, Simek M (2011) Spectrum of sprite halos. *J Geophys Res Space Phys* 116:A09319. <https://doi.org/10.1029/2011JA016652>
- Gordillo-Vázquez FJ, Passas M, Luque A, Sánchez J, van der Velde OA, Montanya J (2018) High spectral resolution spectroscopy of sprites: a natural probe of the mesosphere. *J Geophys Res (Atmos)* 123:2336–2346. <https://doi.org/10.1002/2017JD028126>
- Greenberg E, Price C (2004) A global lightning location algorithm based on the electromagnetic signature in the Schumann resonance band. *J Geophys Res (Atmos)* 109:D21111
- Greenberg E, Price C, Yair Y, Haldoupis C, Chanrion O, Neubert T (2009) ELF/VLF signatures of sprite-producing lightning discharges observed during the 2005 EuroSprite campaign. *J Atmos Sol-Terr Phys* 71:1254–1266. <https://doi.org/10.1016/j.jastp.2009.05.005>
- Haldoupis C, Neubert T, Inan US, Mika A, Allin TH, Marshall RA (2004) Subionospheric early VLF signal perturbations observed in one-to-one association with sprites. *J Geophys Res (Space Phys)* 109:A10303. <https://doi.org/10.1029/2004JA010651>
- Haldoupis C, Steiner RJ, Mika Á, Shalimov S, Marshall RA, Inan US, Bösinger T, Neubert T (2006) “Early/slow” events: a new category of VLF perturbations observed in relation with sprites. *J Geophys Res (Space Phys)* 111:A11321. <https://doi.org/10.1029/2006JA011960>
- Haldoupis C, Amvrosiadi N, Cotts BRT, van der Velde OA, Chanrion O, Neubert T (2010) More evidence for a one-to-one correlation between Sprites and Early VLF perturbations. *J Geophys Res (Space Phys)* 115:A07304. <https://doi.org/10.1029/2009JA015165>
- Haldoupis C, Cohen M, Cotts B, Arnone E, Inan U (2012) Long-lasting D-region ionospheric modifications, caused by intense lightning in association with elve and sprite pairs. *Geophys Res Lett* 39:L16801. <https://doi.org/10.1029/2012GL052765>
- Haldoupis C, Cohen M, Arnone E, Cotts B, Dietrich S (2013) The VLF fingerprint of elves: step-like and long-recovery early VLF perturbations caused by powerful CG lightning EM pulses. *J Geophys Res (Space Phys)* 118:5392–5402
- Ignaccolo M, Farges T, Mika A, Allin TH, Chanrion O, Blanc E, Fraser-Smith AC, Füllekrug M (2006) The planetary rate of sprite events. *Geophys Res Lett* 33:L11808. <https://doi.org/10.1029/2005GL025502>
- Ignaccolo M, Farges T, Blanc E, Füllekrug M (2008) Automated chirp detection with diffusion entropy: application to infrasound from sprites. *Chaos Solitons Fractals* 38:1039–1050. <https://doi.org/10.1016/j.chaos.2007.02.011>
- Inan US, Barrington-Leigh C, Hansen S, Glukhov VS, Bell TF, Rairden R (1997) Rapid lateral expansion of optical luminosity in lightning-induced ionospheric flashes referred to as ‘elves’. *Geophys Res Lett* 24:583–586. <https://doi.org/10.1029/97GL00404>
- Iwański R, Odzimek A, Clausen L, Kanawade V, Cnossen I, Edberg N (2009) Meteorological study of the first observation of red sprites from Poland. *Acta Geophys* 57:760–777. <https://doi.org/10.2478/s11600-009-0008-7>
- Krehbiel PR, Riousset JA, Pasko VP, Thomas RJ, Rison W, Stanley MA, Edens HE (2008) Upward electrical discharges from thunderstorms. *Nat Geosci* 1:233. <https://doi.org/10.1038/ngeo162>
- Kuśak A, Młynarczyk J (2011) A new technique for reconstruction of the current moment waveform related to a gigantic jet from the magnetic field component recorded by an ELF station. *Radio Sci* 46:RS2016. <https://doi.org/10.1029/2010RS004475>

- Lefevre F, Blanc E, Pinçon J-L, Roussel-Dupré R, Lawrence D, Sauvaud J-A, Rauch J-L, de Feraudy H, Lagoutte D (2008) TARANIS—a satellite project dedicated to the physics of TLEs and TGFs. *Space Sci Rev* 137:301–315. <https://doi.org/10.1007/s11214-008-9414-4>
- Liszka L, Hobara Y (2006) Sprite-attributed infrasonic chirps—their detection, occurrence and properties between 1994 and 2004. *J Atmos Sol-Terr Phys* 68:1179–1188
- Luque A, Ebert U (2009) Emergence of sprite streamers from screening-ionization waves in the lower ionosphere. *Nature Geosci* 2:757–760. <https://doi.org/10.1038/ngeo662>
- Lyons A (1994) Characteristics of luminous structures in the stratosphere above thunderstorms as imaged by low-light video. *Geophys Res Lett* 21:875–878
- Lyons WA (1996) Sprite observations above the U.S. High Plains in relation to their parent thunderstorm systems. *J Geophys Res* 101:29641–29652
- Mäkelä A, Kantola T, Yair Y, Raita T (2010) Observations of TLEs above the Baltic sea on Oct 9 2009. *Geophysica* 46:79–90
- Mika Á, Haldoupis C, Marshall RA, Neubert T, Inan US (2005) Subionospheric VLF signatures and their association with sprites observed during EuroSprite-2003. *J Atmos Sol-Terr Phys* 67:1580–1597. <https://doi.org/10.1016/j.jastp.2005.08.011>
- Mika Á, Haldoupis C, Neubert T, Su HT, Hsu RR, Steiner RJ, Marshall RA (2006) Early VLF perturbations observed in association with elves. *Ann Geophys* 24:2179–2189
- Mlynarczyk J, Bór J, Kulak A, Popek M, Kubisz J (2015) An unusual sequence of sprites followed by a secondary TLE: an analysis of ELF radio measurements and optical observations. *J Geophys Res (Space Phys)* 120:2241–2254. <https://doi.org/10.1002/2014JA020780>
- Montanya J, van der Velde O, Romero D, March V, Solà G, Pineda N, Arrayas M, Trueba JL, Reglero V, Soula S (2010) High-speed intensified video recordings of sprites and elves over the western Mediterranean Sea during winter thunderstorms. *J Geophys Res (Atmos)* 115:A00E18. <https://doi.org/10.1029/2009JA014508>
- NaitAmor S, AlAbdoadain MA, Cohen MB, Cotts BRT, Soula S, Chanrion O, Neubert T, Abdelatif T (2010) VLF observations of ionospheric disturbances in association with TLEs from the Euro-Sprite-2007 campaign. *J Geophys Res (Space Phys)* 115:A00E47. <https://doi.org/10.1029/2009JAO15026>
- Neubert T (2003) On sprites and their exotic kin. *Science* 300:747–749
- Neubert T (2009) ASIM—an Instrument Suite for the International Space Station. In: American Institute of Physics Conference Series, vol. 1118 of American Institute of Physics Conference Series, pp 8–12. <https://doi.org/10.1063/1.3137718>
- Neubert T, Chanrion O (2013) On the electric breakdown field of the mesosphere and the influence of electron detachment. *Geophys Res Lett* 40:2373–2377. <https://doi.org/10.1002/grl.50433>
- Neubert T, Allin TH, Stenbaek-Nielsen H, Blanc E (2001) Sprites over Europe. *Geophys Res Lett* 28:3585–3588
- Neubert T, Allin TH, Blanc E, Farges T, Haldoupis C, Mika A, Soula S, Knutsson L, van der Velde O, Marshall RA, Inan U, Sátorí G, Bór J, Hughes A, Collier A, Laursen S, Rasmussen I (2005) Coordinated observations of transient luminous events during the EuroSprite2003 campaign. *J Atmos Sol-Terr Phys* 67:807–820. <https://doi.org/10.1016/j.jastp.2005.02.004>
- Neubert T, Rycroft M, Farges T, Blanc E, Chanrion O, Arnone E, Odzimek A, Arnold N, Enell C-F, Turunen E, Bösinger T, Mika Á, Haldoupis C, Steiner RJ, van der Velde O, Soula S, Berg P, Boberg F, Thejll P, Christiansen B, Ignaccolo M, Füllekrug M, Veronen PT, Montanya J, Crosby N (2008) Recent results from studies of electric discharges in the mesosphere. *Surv Geophys* 29:71. <https://doi.org/10.1007/s10712-008-9043-1>
- Neubert T, Chanrion O, Arnone E, Zanotti F, Cummer S, Li J, Füllekrug M, Soula S, van der Velde O (2011) The properties of a gigantic jet reflected in a simultaneous sprite: observations interpreted by a model. *J Geophys Res (Space Phys)* 116:A12329. <https://doi.org/10.1029/2011JA016928>
- Neubert T, Østgaard N, Reglero V, Blanc E, Chanrion O, Oxborrow CA, Orr A, Tacconi M (2019) The ASIM mission on the International Space Station. *Space Sci Rev* 215:26. <https://doi.org/10.1007/s11214-019-0592-z>
- Newsome RT, Inan US (2010) Free-running ground-based photometric array imaging of transient luminous events. *J Geophys Res (Space Phys)* 115:A00E41
- Odzimek A, Clausen LBN, Kanawade V, Cnossen I, Edberg NJT, Faedi F, Del Moro A, Ural U, Byckling K, Krzaczkowski P, Iwański R, Struzik P, Pajek M, Gajda W (2008) SPARTAN Sprite-Watch 2007 Campaign. In: Choliy VY, Ivashchenko G (eds) Young scientists 15th proceedings, pp 64–67
- Parra-Rojas FC, Luque A, Gordillo-Vázquez FJ (2013) Chemical and electrical impact of lightning on the Earth mesosphere: the case of sprite halos. *J Geophys Res (Space Phys)* 118:5190–5214. <https://doi.org/10.1002/jgra.50449>


- Parra-Rojas FC, Luque A, Gordillo-Vázquez FJ (2015) Chemical and thermal impacts of sprite streamers in the Earth's mesosphere. *J Geophys Res (Space Phys)* 120:8899–8933
- Pasko VP (2008) Blue jets and gigantic jets: transient luminous events between thunderstorm tops and the lower ionosphere. *Plasma Phys Controll Fusion* 50:124050. <https://doi.org/10.1088/0741-3335/50/12/124050>
- Pasko VP (2010) Recent advances in theory of transient luminous events. *J Geophys Res (Space Phys)* 115:A00E35
- Pasko VP, Inan US, Bell TF (1997) Sprite as evidence of vertical gravity wave structures above mesoscale thunderstorms. *Geophys Res Lett* 24:1735–1738
- Pasko VP, Inan US, Bell TF (1998) Spatial structure of sprites. *Geophys Res Lett* 25:2123–2126
- Pasko VP, Stanley MA, Mathews JD, Inan US, Wood TG (2002) Electrical discharge from a thundercloud top to the lower ionosphere. *Nature* 416:152–154
- Pasko VP, Yair Y, Kuo CL (2011) Lightning related transient luminous events at high altitude in the Earth's atmosphere: phenomenology, mechanisms and effects. *Space Sci Rev.* <https://doi.org/10.1007/s11214-011-9813-9>
- Pérez-Invernón FJ, Luque A, Gordillo-Vázquez FJ (2018a) Modeling the chemical impact and the optical emissions produced by lightning-induced electromagnetic fields in the upper atmosphere: the case of halos and elves triggered by different lightning discharges. *J Geophys Res (Atmos)* 123:7615–7641. <https://doi.org/10.1029/2017JD028235>
- Pérez-Invernón FJ, Luque A, Gordillo-Vázquez FJ, Sato M, Ushio T, Adachi T, Chen AB (2018b) Spectroscopic diagnostic of halos and elves detected from space-based photometers. *J Geophys Res (Atmos)* 123:12917–12941. <https://doi.org/10.1029/2018JD029053>
- Pérez-Invernón FJ, Gordillo-Vázquez FJ, Smith AK, Arnone E, Winkler H (2019) Global occurrence and chemical impact of stratospheric blue jets modeled with WACCM4. *J Geophys Res (Atmos)* 124:2841–2864. <https://doi.org/10.1029/2018JD029593>
- Petrov NI, Petrova GN (1999) Physical mechanisms for the development of lightning discharges between a thundercloud and the ionosphere. *J Tech Phys* 44:472–475. <https://doi.org/10.1134/1.1259327>
- Pinto CMA, Mendes Lopes A, Machado JAT (2012) A review of power laws in real life phenomena. *Commun Nonlinear Sci Numer Simul* 17:3558–3578. <https://doi.org/10.1016/j.cnsns.2012.01.013>
- Price C, Asfur M, Lyons W, Nelson T (2002) An improved ELF/VLF method for globally geolocating sprite-producing lightning. *Geophys Res Lett* 29:1031. <https://doi.org/10.1029/2001GL013519>
- Rodger CJ (1999) Red sprites, upward lightning, and VLF perturbations. *Rev Geophys* 37:317–336
- Rodger CJ, Werner S, Brundell J, Thomson NR, Lay E, Holzworth R, Dowden R (2006) Detection efficiency of the VLF World-Wide Lightning Location Network (WWLLN): initial case study. *Ann Geophys* 24:3197–3214
- Rudlosky SD, Shea DT (2013) Evaluating WWLLN performance relative to TRMM/LIS. *Geophys Res Lett* 40:2344–2348. <https://doi.org/10.1002/grl.50428>
- Rycroft MJ, Harrison RG (2011) Electromagnetic atmosphere-plasma coupling: the global atmospheric electric circuit. *Space Sci Rev.* <https://doi.org/10.1007/s11214-011-9830-8>
- Rycroft MJ, Odzimek A (2010) Effects of lightning and sprites on the ionospheric potential, and threshold effects on sprite initiation, obtained using an analog model of the global atmospheric electric circuit. *J Geophys Res (Space Phys)* 115:A00E37. <https://doi.org/10.1029/2009JA014758>
- Rycroft MJ, Odzimek A, Arnold NF, Füllekrug M, Kuřak A, Neubert T (2007) New model simulations of the global atmospheric electric circuit driven by thunderstorms and electrified shower clouds: the roles of lightning and sprites. *J Atmos Sol-Terr Phys* 69:2485–2509. <https://doi.org/10.1016/j.jastp.2007.09.004>
- Sátori G, Neska M, Williams E, Szendrői J (2007) Signatures of the day-night asymmetry of the Earth-ionosphere cavity in high time resolution Schumann resonance records. *Radio Sci* 42:RS2S10. <https://doi.org/10.1029/2006RS003483>
- Sátori G, Rycroft M, Bencze P, Märcz F, Bór J, Barta V, Nagy T, Kovács K (2013) An overview of thunderstorm-related research on the atmospheric electric field, Schumann resonances, sprites, and the ionosphere at Sopron, Hungary. *Surv Geophys* 34:255–292. <https://doi.org/10.1007/s10712-013-9222-6>
- Savtchenko A, Mitzeva R, Tsenova B, Kolev S (2009) Analysis of lightning activity in two thunderstorm systems producing sprites in France. *J Atmos Sol-Terr Phys* 71:1277–1286. <https://doi.org/10.1016/j.jastp.2009.04.010>
- Sentman DD, Wescott EM (1993) Observations of upper atmospheric optical flashes recorded from an aircraft. *Geophys Res Lett* 20:2857–2860
- Sentman DD, Wescott EM, Osborne DL, Hampton DL, Heavner MJ (1995) Preliminary results from the Sprites94 aircraft campaign: 1. Red sprites. *Geophys Res Lett* 22:1205–1208
- Smith DM, Lopez LI, Lin RP, Barrington-Leigh CP (2005) Terrestrial gamma-ray flashes observed up to 20 MeV. *Science* 307:1085–1088. <https://doi.org/10.1126/science.1107466>

- Soula S, van der Velde O, Palmiéri J, Chanrion O, Neubert T, Montanya J, Gangneron F, Meyerfeld Y, Lefeuvre F, Lointier G (2010) Characteristics and conditions of production of transient luminous events observed over a maritime storm. *J Geophys Res (Atmos)* 115:D16118. <https://doi.org/10.1029/2009JD012066>
- Soula S, Iacovella F, van der Velde O, Montanya J, Füllekrug M, Farges T, Bór J, Georgis J-F, NaitAmor S, Martin J-M (2014) Multi-instrumental analysis of large sprite events and their producing storm in southern France. *Atmos Res* 135:415–431
- Soula S, Defer E, Füllekrug M, van der Velde O, Montanya J, Bousquet O, Mlynarczyk J, Coquillat S, Pinty J-P, Rison W, Krehbiel PR, Thomas R, Pedebay S (2015) Time and space correlation between sprites and their parent lightning flashes for a thunderstorm observed during the HyMeX campaign. *J Geophys Res (Atmos)* 120:11. <https://doi.org/10.1002/2015JD023894>
- Soula S, Mlynarczyk J, Füllekrug M, Pineda N, Georgis J-F, van der Velde O, Montanya J, Fabró F (2017) Dancing sprites: detailed analysis of two case studies. *J Geophys Res (Atmos)* 122:3173–3192. <https://doi.org/10.1002/2016JD025548>
- Stanley M, Brook M, Krehbiel P, Cummer SA (2000) Detection of daytime sprites via a unique sprite ELF signature. *Geophys Res Lett* 27:871–874. <https://doi.org/10.1029/1999GL010769>
- Stenbaek-Nielsen HC, Moudry DR, Wescott EM, Sentman DD, Sabbas FTS (2000) Sprites and possible mesospheric effects. *Geophys Res Lett* 27:3829–3832
- Stenbaek-Nielsen HC, Haaland R, McHarg MG, Hensley BA, Kanmae T (2010) Sprite initiation altitude measured by triangulation. *J Geophys Res (Space Phys)* 115:A00E12
- Su HT, Hsu RR, Chen AB, Wang YC, Hsiao WS, Lai WC, Lee LC, Sato M, Fukunishi H (2003) Gigantic jets between a thundercloud and the ionosphere. *Nature* 423:974–976
- Suzuki T, Hayakawa M, Michimoto K (2011) Small Winter thunderstorm with sprites and strong positive discharge. *IEEJ Trans Fundam Mater* 131:723–728. <https://doi.org/10.1541/ieejfms.131.723>
- Taylor MJ, Bailey MA, Pautet PD, Cummer SA, Jaugey N, Thomas JN, Solorzano NN, Sao Sabbas F, Holzworth RH, Pinto O, Schuch NJ (2008) Rare measurements of a sprite with halo event driven by a negative lightning discharge over Argentina. *Geophys Res Lett* 35:L14812. <https://doi.org/10.1029/2008GL033984>
- Vadislavsky E, Yair Y, Erlick C, Price C, Greenberg E, Yaniv R, Ziv B, Reicher N, Devir A (2009) Indication for circular organization of column sprite elements associated with Eastern Mediterranean winter thunderstorms. *J Atmos Sol-Terr Phys* 71:1835–1839. <https://doi.org/10.1016/j.jastp.2009.07.001>
- van der Velde OA, Montanya J (2016) Statistics and variability of the altitude of elves. *Geophys Res Lett* 43:5467–5474. <https://doi.org/10.1002/2016GL068719>
- van der Velde OA, Mika Á, Soula S, Haldoupis C, Neubert T, Inan US (2006) Observations of the relationship between sprite morphology and in-cloud lightning processes. *J Geophys Res (Atmos)* 111:D15203
- van der Velde OA, Bór J, Li J, Cummer SA, Arnone E, Zanotti F, Füllekrug M, Haldoupis C, NaitAmor S, Farges T (2010a) Multi-instrumental observations of a positive gigantic jet produced by a winter thunderstorm in Europe. *J Geophys Res (Atmos)* 115:D24301. <https://doi.org/10.1029/2010JD014442>
- van der Velde OA, Montanya J, Soula S, Pineda N, Bech J (2010b) Spatial and temporal evolution of horizontally extensive lightning discharges associated with sprite-producing positive cloud-to-ground flashes in northeastern Spain. *J Geophys Res (Space Phys)* 115:A00E56. <https://doi.org/10.1029/2009JA014773>
- van der Velde OA, Montanya J, Soula S, Pineda N, Mlynarczyk J (2014) Bidirectional leader development in sprite-producing positive cloud-to-ground flashes: origins and characteristics of positive and negative leaders. *J Geophys Res (Atmos)* 119:12. <https://doi.org/10.1002/2013JD021291>
- Wescott EM, Sentman D, Osborne D, Hampton D, Heavner M (1995) Preliminary results from the Sprites94 aircraft campaign. 2. Blue jets. *Geophys Res Lett* 22:1209–1212
- Wescott EM, Stenbaek Nielsen HC, Sentman DD, Heavner MJ, Moudry D, São Sabbas FT (2001) Triangulation of sprites, associated halos and their possible relation to causative lightning and micrometeors. *J Geophys Res* 106:10467–10477
- Whitley T, Füllekrug M, Rycroft M, Bennett A, Wyatt F, Elliott D, Heinson G, Hitchman A, Lewis A, Sefako R, Fourie P, Dyers J, Thomson A, Flower S (2011) Worldwide extremely low frequency magnetic field sensor network for sprite studies. *Radio Sci* 46:RS4007. <https://doi.org/10.1029/2010RS004523>
- Williams E, Kuo C-L, Bór J, Satori G, Newsome R, Adachi T, Boldi R, Chen A, Downes E, Hsu RR, Lyons W, Saba MMF, Taylor M, Su HT (2012) Resolution of the sprite polarity paradox: the role of halos. *Radio Sci* 47:RS2002. <https://doi.org/10.1029/2011RS004794>
- Winkler H, Notholt J (2014) The chemistry of daytime sprite streamers—a model study. *Atmos Chem Phys* 14:3545–3556. <https://doi.org/10.5194/acp-14-3545-2014>
- Winkler H, Notholt J (2015) A model study of the plasma chemistry of stratospheric Blue Jets. *J Atmos Sol-Terr Phys* 122:75–85. <https://doi.org/10.1016/j.jastp.2014.10.015>

- Yair Y, Price C, Ganot M, Greenberg E, Yaniv R, Ziv B, Sherez Y, Devir A, Bór J, Sátor G (2009) Optical observations of transient luminous events associated with winter thunderstorms near the coast of Israel. *Atmos Res* 91:529–537
- Yair Y, Price C, Katzenelson D, Rosenthal N, Rubanenko L, Ben-Ami Y, Arnone E (2015) Sprite climatology in the Eastern Mediterranean Region. *Atmos Res* 157:108–118. <https://doi.org/10.1016/j.atmosres.2014.12.018>

Publisher's Note Springer Nature remains neutral with regard to jurisdictional claims in published maps and institutional affiliations.

Affiliations

Enrico Arnone^{1,2}  · **József Bór**³ · **Olivier Chanrion**⁴ · **Veronika Barta**³ · **Stefano Dietrich**² · **Carl-Fredrik Enell**⁵ · **Thomas Farges**⁶ · **Martin Füllekrug**⁷ · **Antti Kero**⁸ · **Roberto Labanti**⁹ · **Antti Mäkelä**¹⁰ · **Keren Mezuman**^{11,12} · **Anna Odzimek**¹³ · **Martin Popek**¹⁴ · **Marco Prevedelli**¹⁵ · **Marco Ridolfi**^{15,16} · **Serge Soula**¹⁷ · **Diego Valeri**¹⁸ · **Oscar van der Velde**¹⁹ · **Yoav Yair**²⁰ · **Ferruccio Zanotti**⁹ · **Przemyslaw Zoladek**²¹ · **Torsten Neubert**⁴

¹ Dipartimento di Fisica, Università di Torino, Via Pietro Giuria, 1, 10125 Turin, Italy

² Istituto di Scienza dell'Atmosfera e del Clima – CNR, Turin, Italy

³ Research Centre for Astronomy and Earth Sciences, GGI, Hungarian Academy of Sciences, Sopron, Hungary

⁴ DTU Space, Technical University of Denmark, Kongens Lyngby, Denmark

⁵ EISCAT Scientific Association, Kiruna, Sweden

⁶ CEA, DAM, DIF, 91297 Arpajon, France

⁷ Department of Electronic and Electrical Engineering, University of Bath, Bath, UK

⁸ Sodankylä Geophysical Observatory, University of Oulu, Sodankylä, Finland

⁹ Italian Meteor and TLE Network (IMTN), Bologna, Italy

¹⁰ Finnish Meteorological Institute, Helsinki, Finland

¹¹ Earth and Environmental Sciences, Columbia University, New York, NY, USA

¹² NASA Goddard Institute for Space Studies, New York, NY, USA

¹³ Institute of Geophysics, Polish Academy of Sciences, Warsaw, Poland

¹⁴ Department of Space Physics, Station Nýdek, Institute of Atmospheric Physics, CAS, Prague, Czech Republic

¹⁵ Department of Physics and Astronomy, University of Bologna, Bologna, Italy

¹⁶ Istituto Nazionale di Ottica - CNR, Florence, Italy

¹⁷ Laboratory of Aerology, University of Toulouse/CNRS, Toulouse, France

¹⁸ Department of Civil and Environmental Engineering, Sapienza, Università di Roma, Rome, Italy

¹⁹ Universitat Politècnica de Catalunya, Barcelona, Spain

²⁰ School of Sustainability, Interdisciplinary Center (IDC) Herzliya, Herzliya, Israel

²¹ Comets and Meteors Workshop, Bartycka, Warsaw, Poland